THE GEOMAGNETIC FIELD'S CONFIGURATION OVER THE JAPANESE ISLANDS AT THE TIME WHEN THE ASO-4 TEPHRA WAS DEPOSITED

Junko FUJII[1], Tadashi NAKAJIMA[1] and Kimio HIROOKA[2]

[1] Geological Laboratory, Faculty of Education and Regional Studies, Fukui University, Fukui 910-8507, Japan
[2] Department of Earth Sciences, Faculty of Science, Toyama University, Toyama 930-8555, Japan

ABSTRACT

The Aso pyroclastic-flow deposits, products of major Pleistocene volcanic eruptions in Japan, are divided into four eruptive units: Aso-1, Aso-2, Aso-3, and Aso-4 in ascending order. The paleomagnetic directions determined from welded tuff samples of these units, which are distributed near the source caldera in central Kyushu, are characteristic of the individual units and are all of normal polarity. The unit-mean directions for Aso-1 and Aso-4 are similar to the direction of the present geomagnetic field. The direction for Aso-2 is characterized by an unusually steep inclination, and that for Aso-3 by an unusually easterly declination.

The mean VGP for the Aso-4 co-ignimbrite ash-fall deposits in Chubu, Tohoku, and Hokkaido is identical to those for subunits of the Aso-4 tephra: the Aso-4A welded tuff in Oita Prefecture, the lower part of the Ube volcanic ash layer in Yamaguchi Prefecture, and the distal ash-flow deposit in Miyazaki Prefecture. From the identical VGPs together with stratigraphic evidence, the subunits are inferred to have been deposited at the same time. This indicates that its magnetization was acquired in a geomagnetic field dominated by the same dipole field (DF) component in all regions of the Japanese Islands; the DF pole is inferred to coincide with the overall mean VGP (A_{95}=1.3°, N=42) located at 22.7°W, 83.8°N.

In order to clarify the configuration of the geomagnetic field at the time of the Aso-4A eruption, the surveyed area was divided into eight regions, and the local geomagnetic field (LF) direction of each region was calculated from the regional-mean VGP. Local geomagnetic anomalies, exceeding the α_{95}s of the LF directions, could not be detected by comparing DF and LF in all of the eight regions.

Key words: paleomagnetism, Aso-4 tephra, geomagnetic field's configuration, Aso pyroclastic-flow deposit, Late Pleistocene

藤井純子・中島正志・広岡公夫（2002）阿蘇4テフラ堆積時の日本列島における地磁気分布. 福井県立恐竜博物館紀要 1: 63-91.

　阿蘇火砕流堆積物は4つのユニット（下位から順に Aso-1, -2, -3, -4）に分けられる．これらのユニットから採取された溶結凝灰岩試料の古地磁気方位は，各ユニットで特徴的であり，すべて正帯磁であった．Aso-1 と Aso-4のユニット平均磁化方位は現在の地球磁場方位とよく似ている．Aso-2 の方位は非常に深い伏角によって，Aso-3の方位は極端に東偏する偏角によって特徴づけられる．

　中部，東北および北海道の阿蘇4降下火山灰堆積物の平均 VGP は，大分県の Aso-4A 溶結凝灰岩，山口県の宇部火山灰層下部および宮崎県の遠方火山灰流堆積物のそれらと同じであった．そのような VGP の同一性は，それらの磁化が日本列島全域において同じ双極子磁場（DF）成分が優勢な地球磁場中で獲得されたことを示し，その DF の極は全 VGP の平均（23.7°W，83.7°E，A_{95} = 1.4°，N = 37）の位置にあったと考えられる．

　Aso-4A 噴出時に日本列島で地域磁気異常が存在するかどうかを確かめるために，日本列島を7つの地域に分け検討したが，地域平均磁場方位のα_{95}を越える地域磁気異常は認められなかった．

Junko FUJII: fujii@edu00.f-edu.fukui-u.ac.jp;

Tadashi NAKAJIMA: nakajima@edu00.f-edu.fukui-u.ac.jp;

Kimio HIROOKA: hirooka@sci.toyama-u.ac.jp

1. INTRODUCTION

Aso caldera in central Kyushu of the Japanese Islands is one of the largest calderas in the world and covers an area of 380 km². In middle to late Pleistocene time, eruptions of voluminous pyroclastic flows occurred intermittently, resulting in formation of the caldera. The Aso pyroclastic-flow deposits are divided into four major units, i.e. Aso-1, Aso-2, Aso-3, and Aso-4 in ascending order (Ono et al., 1977). Welded tuffs of these units are voluminous, and are widely distributed in central Kyushu. Paleomagnetic measurements have been made on samples of these welded tuffs, which are generally well suited for paleomagnetic research, from many sites to determine precise geomagnetic field directions at each time of eruption for the four major units. K-Ar ages of Aso-1, Aso-2, Aso-3, and Aso-4 were determined to be 266±14 ka, 141±5 ka, 123±6 ka, and 89±7 ka, respectively (Matsumoto et al., 1991).

In order to construct geomagnetic charts for the Japanese Islands in prehistoric times, we have been carrying out paleomagnetic studies of widespread late Pleistocene tephras (Nakajima and Fujii, 1995a, 1995b, 1998; Fujii and Nakajima, 1998; Fujii et al., 2000, 2001). Nakajima and Fujii (1995a) made paleomagnetic measurements on the Aira Tn tephra (AT), which erupted from Aira caldera at about 25 ka and spread over distances of at least 1,400 km from southern Kyushu to Tohoku (Machida and Arai, 1992). Using stable paleomagnetic directions from AT at 44 sites, isogonic and isoclinic charts for the time of eruption (Figs. 1 and 2) were constructed. The magnetic charts show that declination in the Okayama-Hiroshima region is deflected westerly by about 5° from those in the nearby regions, and inclination in the Toyama region is steeper by about 7° than those in the nearby regions. These anomalous directions were thought to have been caused by past geomagnetic anomalies due to non-dipole component.

Fujii and Nakajima (1998) presented paleomagnetic directions for several other widespread tephras, including the Kikai-Akahoya, the Daisen-Kurayoshi, the Aso-4, and the Sambe-Kisuki tephras (Machida and Arai, 1992). Each tephra showed a characteristic paleomagnetic direction, presumably the geomagnetic field direction recorded at the time of eruption (Fig. 3). The number of measurements is still too few, however, to discuss the geomagnetic field's exact configuration at the time each tephra was deposited over the Japanese Islands.

Co-ignimbrite ashes-fall deposits of Aso-1, Aso-3, and Aso-4 have been found in multiple areas of the Japanese Islands (Japan Assoc. Quaternary Res., 1996). The Aso-4 co-ignimbrite ash-fall deposit, especially, has been described by many stratigraphic researchers (e.g., Machida et al., 1985; Suzuki et al., 1995), and is one of the most famous ashes of late Quaternary age in Japan. In this study paleomagnetic samples were intensively collected from the Aso-4 co-ignimbrite ash-fall deposit. Preliminary reports of the Aso pyroclastic-flow and the Aso-4 co-ignimbrite ash-fall deposits' paleomagnetism were presented by Nakajima

and Fujii (1998), and Fujii et al. (2000, 2001). In this paper, we discuss the geomagnetic field at the time the Aso pyroclastic-flow deposits were deposited, and especially when the Aso-4 tephra was deposited, on the basis of all the paleomagnetic data obtained so far.

2. SAMPLES

We collected paleomagnetic samples in central Kyushu from welded tuffs of proximal facies of four major units: Aso-1, Aso-2, Aso-3, and Aso-4. As for Aso-4, not only was welded tuff sampled, but also ash-flow deposits of the distal facies were collected in southern Kyushu and Chugoku (Table 1, Fig. 4). Moreover, we collected the Aso-4 co-ignimbrite ash-fall deposit in Chubu, Tohoku, and Hokkaido.

2.1 Welded tuffs of the Aso pyroclastic-flow deposits

The rocks of Aso-1, Aso-2, and Aso-3 are of pyroxene rhyolite and andesite, while those of Aso-4 are hypersthene-hornblende rhyolite with small amounts of pyroxene-hornblende andesite (Ono et al., 1977).

Welded tuff samples of Aso-1 and Aso-2 were collected chiefly in the Aso caldera wall and in the Miyanoharu district of Kumamoto Prefecture, based on the 1:50,000 geological maps of Ono and Watanabe (1985), and Kamata (1997). Although Aso-2 is divided into two subunits: Aso-2A and Aso-2B in ascending order, samples were collected only from Aso-2A which occurs mostly as densely welded tuff.

Samples of Aso-3 and Aso-4 were collected mainly in the Taketa district of Oita Prefecture, based on the 1:50,000 geological map of Ono et al. (1977). Aso-3 and Aso-4 in the Taketa district are divided into three subunits (Aso-3A, Aso-3B, and Aso-3C), and into two subunits (Aso-4A and Aso-4B), respectively. We collected oriented samples from all of the subunits, except Aso-3C whose welded parts were rarely exposed in the district.

Ten hand samples were collected from each site, and were oriented with a magnetic compass. The orientation azimuth was corrected for local declination of the present geomagnetic field, based on the values given in the isogonic chart for 1990.0 of the Geographical Survey Institute of Japan (National Astronomical Observatory, 1999). Two or more cylindrical specimens of 25 mm in diameter and 25 mm in height were drilled from each oriented sample, and a total of 20 to 25 specimens were obtained from each site.

2.2 The Aso-4 pyroclastic-flow deposit

Aso-4 is divided into several subunits in each district of the source area (Hoshizumi et al.,1988; Teraoka and Okumura et al., 1990; Teraoka and Miyazaki et al., 1992; Sakai et al., 1993; Kamata, 1997). For instance, Aso-4 is divided into eight subunits from the Oyatsu white pumice-flow to the Kunomine scoria-flow deposits in the Kumamoto district, and is divided
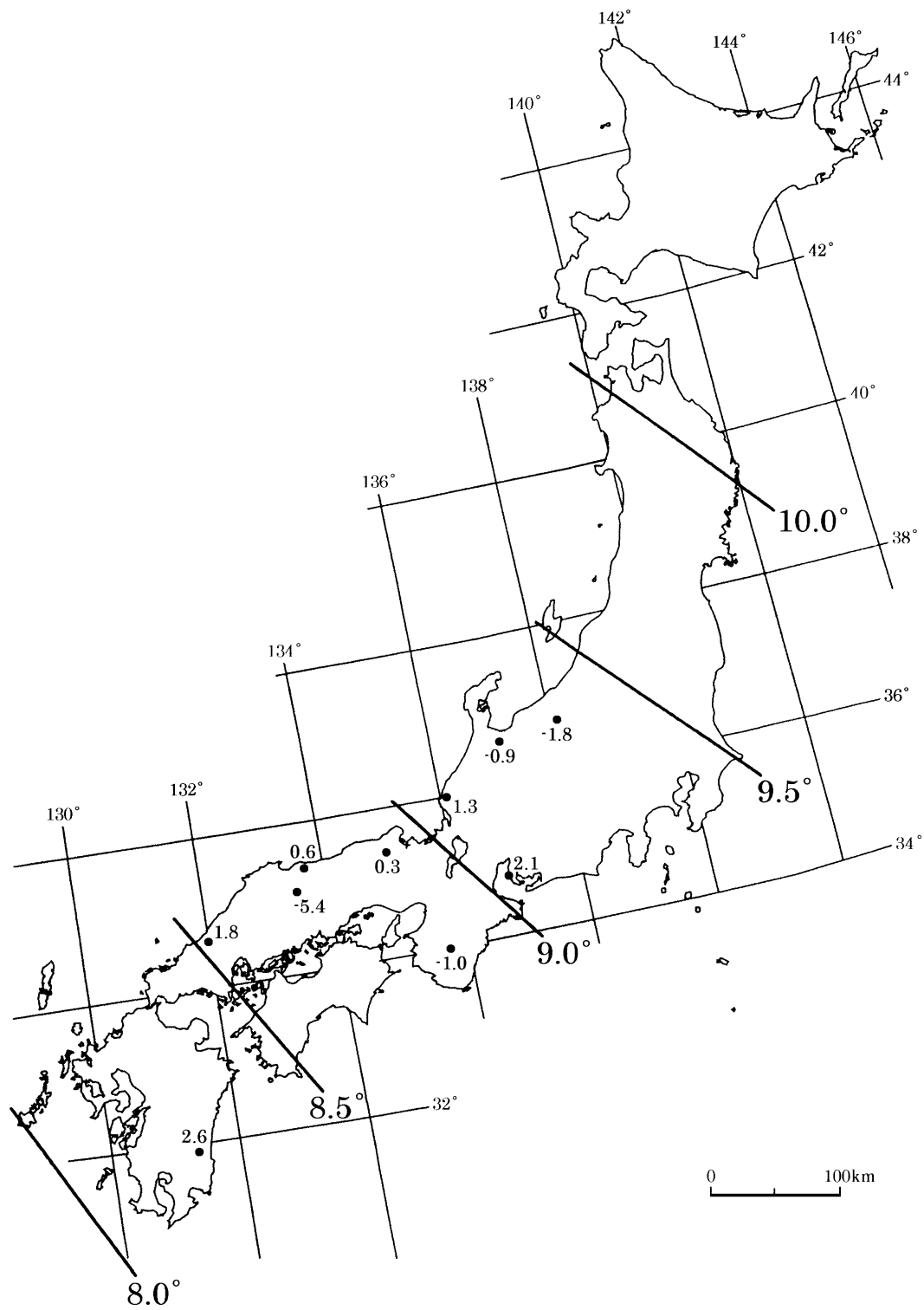
FIGURE 1. Isogonic chart at the time of the AT eruption (after Nakajiama and Fujii, 1995a). Isogonic lines are calculated from the overall-mean VGP. The surveyed area was divided into ten regions. Solid circles show representative points in the individual regions. Numbers adjacent to the solid circles show declination differences between the local and dipole geomagnetic fields at the representative points.
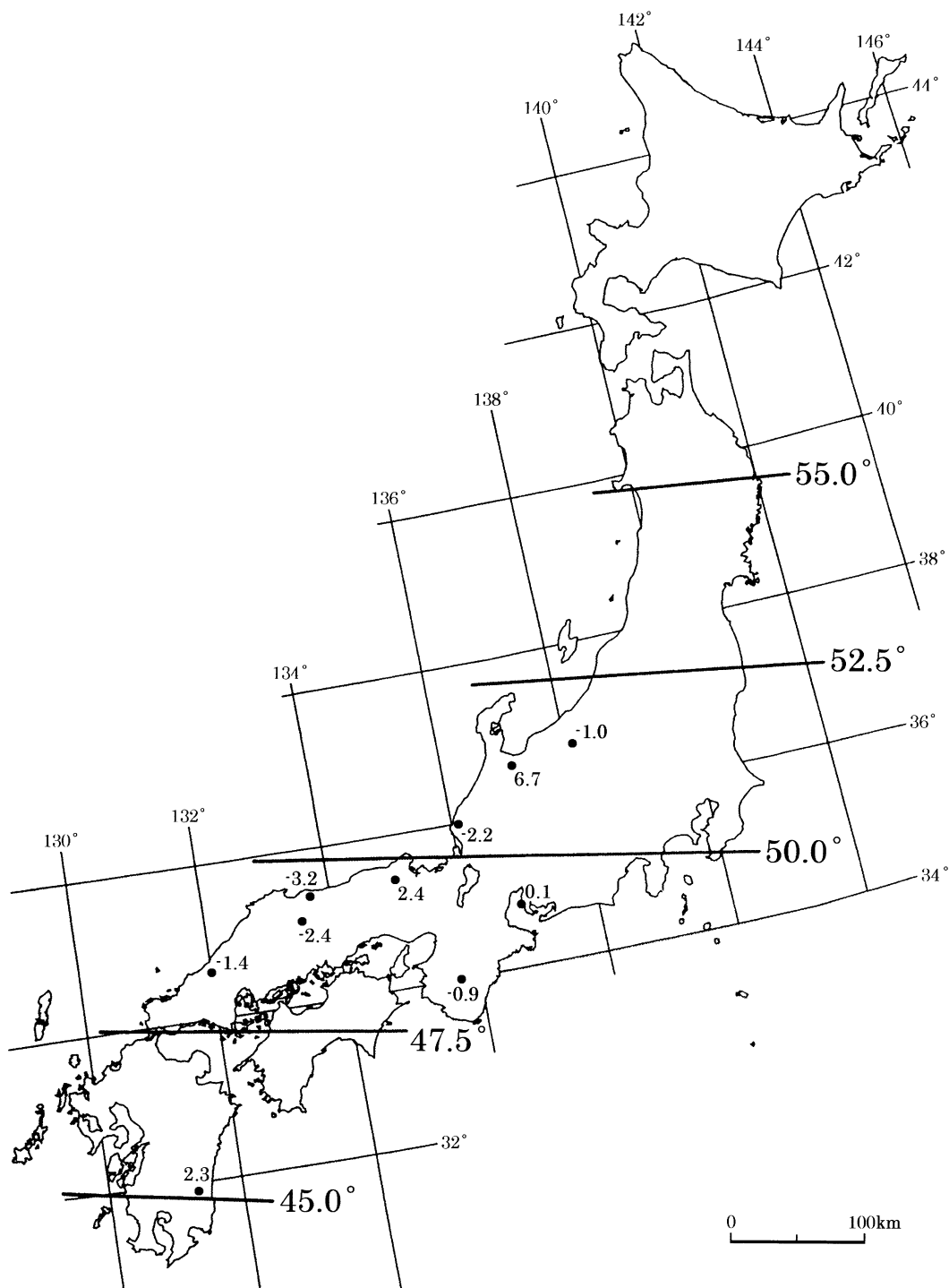
FIGURE 2. Isoclinic chart at the time of the AT eruption (after Nakajima and Fujii, 1995a). Isoclinic lines are calculated from the overall-mean VGP. The surveyed area was divided into ten regions. Solid circles show representative points in the individual regions. Numbers adjacent to the solid circles show inclination differences between the local and dipole geomagnetic fields at the representative points.
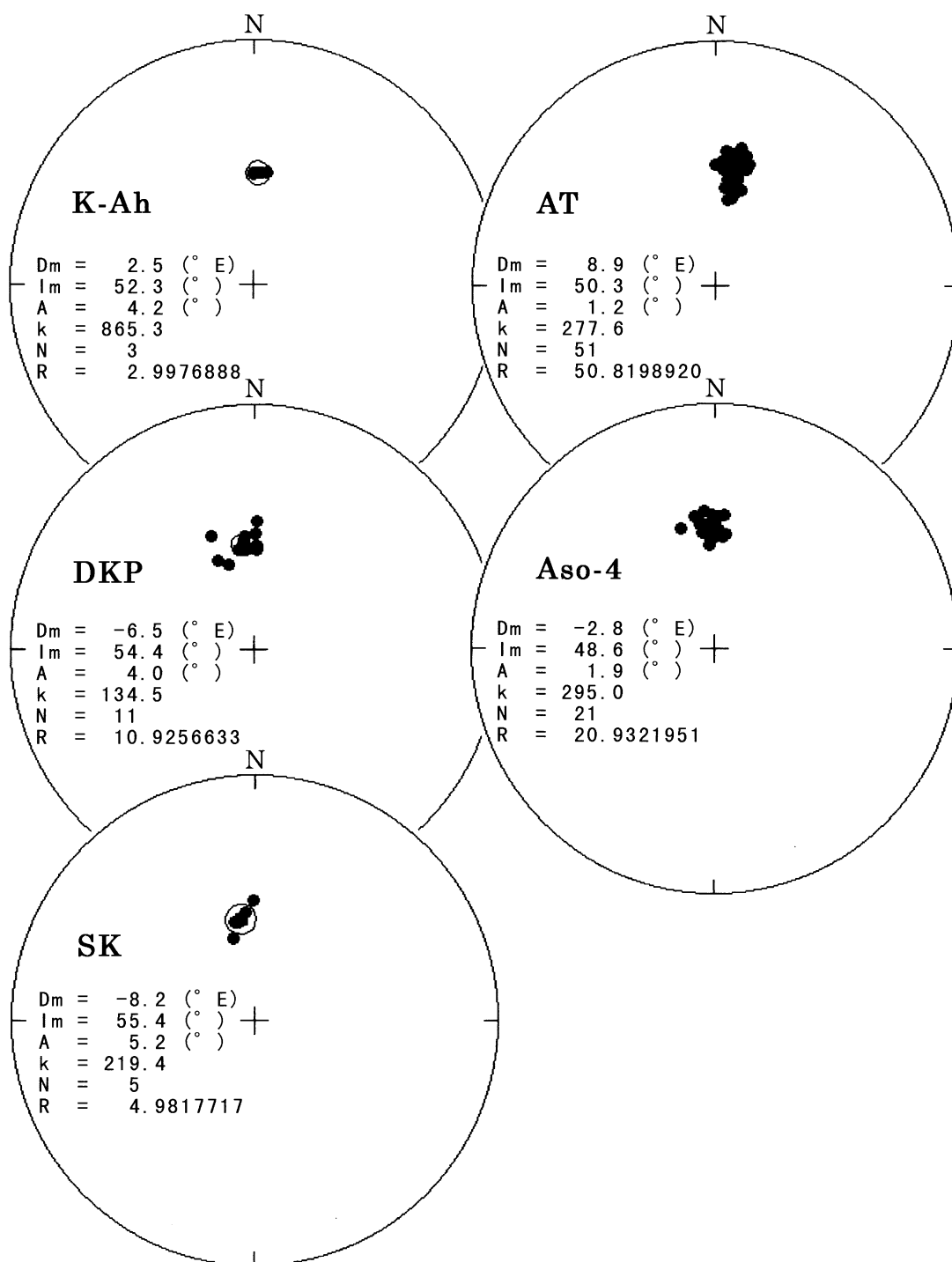
FIGURE 3. Equal-area projections showing site-mean paleomagnetic directions for the Kikai-Akahoya (K-Ah), the Aira Tn (AT), the Daisen-Kurayoshi (DKP), the Aso-4 (Aso-4), and the Sambe-Kisuki (SK) tephras (after Fujii and Nakajima, 1998). Numerical values on the projections show tephra-mean directions. Circles of 95% confidence are for the tephra-mean directions.

TABLE 1. Sampling localities. References are to papers describing the location and geologic setting of each site. Sampling sites are also shown in Fig. 4.

Site	Locality	Longitude, Latitude	Reference
Welded tuff			
Aso-4B			
4B1	Sakuramachi	131°17′ 47.7″ E, 32°54′ 57.6″ N	Ono et al. (1977)
4B2	Ikebe-1	131°16′ 40.4″ E, 32°57′ 56.4″ N	Ono et al. (1977)
4B3	Amakunugi	131°16′ 39.5″ E, 32°57′ 01.1″ N	Ono et al. (1977)
4B4	Shindo	131°16′ 39.5″ E, 32°57′ 01.1″ N	Ono et al. (1977)
4B5	Ikebe-2	131°16′ 23.8″ E, 32°57′ 46.3″ N	Ono et al. (1977)
4B6	Miyabira	131°15′ 18.4″ E, 32°53′ 39.5″ N	Ono et al. (1977)
Aso-4A			
4A1	Harajiri	131°27′ 14.9″ E, 32°57′ 41.0″ N	Ono et al. (1977)
4A2	Namese	131°24′ 31.7″ E, 32°57′ 44.2″ N	Ono et al. (1977)
4A3	Madokoro	131°23′ 23.1″ E, 32°59′ 05.5″ N	Ono et al. (1977)
4A4	Shichiri	131°24′ 24.9″ E, 32°58′ 15.9″ N	Ono (1996a)
4A5	Taketa 1	131°24′ 02.7″ E, 32°57′ 58.0″ N	Ono (1996b)
4A6	Yunoharu	131°23′ 09.6″ E, 33°03′ 45.2″ N	Ono (1996c)
4A7	Taketa 2	131°24′ 00.6″ E, 32°57′ 58.9″ N	Ono et al. (1977)
4A8	Uetsuno	131°23′ 47.1″ E, 32°57′ 18.2″ N	Ono et al. (1977)
Aso-3B			
3B1	Deai 1	131°21′ 00.4″ E, 32°54′ 14.5″ N	Ono et al. (1977)
3B2	Deai 2	131°20′ 56.5″ E, 32°54′ 12.8″ N	Ono et al. (1977)
3B3	Shichiri	131°24′ 24.9″ E, 32°58′ 15.9″ N	Ono (1996a)
3B4	Nakao	131°23′ 07.5″ E, 32°56′ 14.8″ N	Ono et al. (1977)
3B5	Sarukuchi	131°22′ 19.4″ E, 32°56′ 12.4″ N	Ono et al. (1977)
3B6	Ibuse	131°21′ 08.1″ E, 32°54′ 59.0″ N	Ono et al. (1977)
Aso-3A			
3A1	Yanagidani	131°10′ 11.5″ E, 32°48′ 32.2″ N	Ono et al. (1977)
3A2	Nagano	131°17′ 13.0″ E, 32°51′ 33.5″ N	Ono et al. (1977)
3A3	Futamata	131°19′ 54.9″ E, 32°51′ 48.1″ N	Ono et al. (1977)
Aso-2A			
2A1	Shiroyama	131°08′ 26.0″ E, 32°58′ 25.7″ N	Ono (1965)
2A2	Takimurozaka	131°08′ 39.5″ E, 32°56′ 16.4″ N	Ono (1965)
2A3	Kikawa 1	131°04′ 58.4″ E, 33°02′ 30.4″ N	Kamata (1997)
2A4	Kikawa 2	131°04′ 47.8″ E, 33°02′ 40.2″ N	Kamata (1997)
2A5	Takinokuchi	131°04′ 41.0″ E, 33°03′ 16.3″ N	Kamata (1997)
2A6	Tonashi	131°04′ 30.9″ E, 33°04′ 10.8″ N	Kamata (1997)
Aso-1			
1-1	Taketa	131°24′ 02.7″ E, 32°57′ 58.0″ N	Ono (1996b)
1-2	Kikuchi-keikoku	130°57′ 13.9″ E, 32°59′ 50.2″ N	Ono & Watanabe (1985)
1-3	Shinbashi 1	131°03′ 46.0″ E, 33°07′ 14.1″ N	Kamata (1997)
1-4	Shinbashi 2	131°03′ 51.8″ E, 33°07′ 23.9″ N	Kamata (1997)
1-5	Shiroyama	131°09′ 41.0″ E, 32°58′ 21.6″ N	Ono (1965)

TABLE 1. (continued)

| Site	Locality	Longitude, Latitude	Reference
Aso-4T pumice-flow deposit			
4T1	Hijyudai	131°18′ 17.4″ E, 33°19′ 17.0″ N	Hoshizumi *et al.* (1988)
4T2	Taniinuyama	131°30′ 59.9″ E, 33°02′ 08.1″ N	Teraoka *et al.* (1992)
Aso-4A pyroclastic-flow deposit (non-welded)			
4A9	Osako	131°36′ 35.9″ E, 33°02′ 50.3″ N	Teraoka *et al.* (1992)
Yame clay			
4A10	Nakamasunaga	130°26′ 29.0″ E, 32°58′ 11.0″ N	Gohara *et al.* (1964)
4A11	Takahama	130°27′ 28.0″ E, 32°56′ 36.0″ N	Gohara *et al.* (1964)
Aso-4 distal ash-flow deposit			
(Yamaguchi Prefecture)			
PY1L, PY1U	Sumouba	131°23′ 54.1″ E, 34°19′ 15.8″ N	Fujii *et al.* (2000)
PY2L, PY2U	Shibao	131°17′ 41.9″ E, 34°16′ 26.9″ N	Fujii *et al.* (2000)
PY3L	Tanoono	131°17′ 27.1″ E, 34°02′ 47.8″ N	Fujii *et al.* (2000)
PY4L, PY4U	Oka	131°20′ 38.0″ E, 34°00′ 43.8″ N	Fujii *et al.* (2000)
PY5L, PY5U	Iwanagaichi	131°17′ 44.0″ E, 34°10′ 54.5″ N	Fujii *et al.* (2000)
PY6U	Ogawa	131°20′ 29.4″ E, 34°15′ 44.3″ N	Fujii *et al.* (2000)
PY7U	Matsubara	131°21′ 12.1″ E, 34°16′ 07.1″ N	Fujii *et al.* (2000)
PY8L, PY8U	Nitanda	131°21′ 30.0″ E, 34°17′ 36.1″ N	Fujii *et al.* (2000)
PY9U	Shinmachihigashikami	131°24′ 03.4″ E, 34°06′ 49.3″ N	Fujii *et al.* (2000)
PY10L	Hanaga	131°19′ 02.1″ E, 34°05′ 51.2″ N	Fujii *et al.* (2000)
PY11L, PY11U	Arase	131°17′ 46.6″ E, 34°03′ 33.5″ N	Fujii *et al.* (2000)
PY12L, PY12U	Senzai	131°20′ 00.2″ E, 33°59′ 47.8″ N	Fujii *et al.* (2000)
PY13U	Hamaomote	131°20′ 19.1″ E, 34°00′ 05.7″ N	Fujii *et al.* (2000)
(Miyazaki Prefecture)			
PM1	Kunitomi	131°18′ 31.6″ E, 32°01′ 30.7″ N	Endo & Suzuki (1986)
PM2	Tonokoori 1	131°23′ 15.0″ E, 32°03′ 12.7″ N	Endo & Suzuki (1986)
PM3	Tonokoori 2	131°22′ 34.3″ E, 32°02′ 59.9″ N	Endo & Suzuki (1986)
PM4	Chugenbaru	131°24′ 27.8″ E, 32°02′ 41.8″ N	Endo & Suzuki (1986)
PM5	Heda	131°33′ 12.0″ E, 32°11′ 06.7″ N	Endo & Suzuki (1986)
Aso-4 co-ignimbrite ash-fall deposit			
AS1	Kurosaki	136°17′ 38.7″ E, 36°20′ 15.4″ N	Toyokura *et al.* (1991)
AS2	Takano	138°02′ 37.4″ E, 36°32′ 48.3″ N	Kimura (1996)
AS3	Uenohara	139°07′ 37.0″ E, 35°36′ 18.6″ N	Yonezawa *et al.* (1996)
AS4	Oyama	139°00′ 05.0″ E, 35°22′ 25.9″ N	Machida (1996)
AS5	Nishinasuno	139°58′ 35.1″ E, 36°54′ 27.6″ N	Suzuki (1993)
AS6	Hayama	140°05′ 47.7″ E, 37°33′ 55.8″ N	Suzuki *et al.* (1995)
AS7	Hibara-ko	140°02′ 55.9″ E, 37°39′ 39.7″ N	Suzuki *et al.* (1995)
AS8	Naruko	140°44′ 26.6″ E, 38°49′ 27.5″ N	Yagi & Soda (1989)
AS9	Koshimizu	144°26′ 36.0″ E, 43°53′ 59.7″ N	
AS10	Abashiri	144°23′ 06.3″ E, 43°51′ 07.9″ N	Okumura (1996)
AS11	Memanbetsu	144°09′ 12.0″ E, 43°52′ 36.9″ N	
AS12	Asanai	140°02′ 30.5″ E, 40°08′ 58.4″ N	
AS13	Yasuda	139°51′ 03.5″ E, 39°58′ 09.2″ N	Shiraishi *et al.* (1992)
AS14	Ikadachi	135°52′ 54.8″ E, 35°08′ 05.6″ N	Kimura *et al.* (1998)
AS15	Shigaraki	136°04′ 01.3″ E, 34°55′ 19.5″ N	
AS16	Miho	138°42′ 08.3″ E, 36°58′ 40.3″ N	Watanabe *et al.* (1999)
AS17	Oyachi	138°36′ 46.1″ E, 36°56′ 50.3″ N	
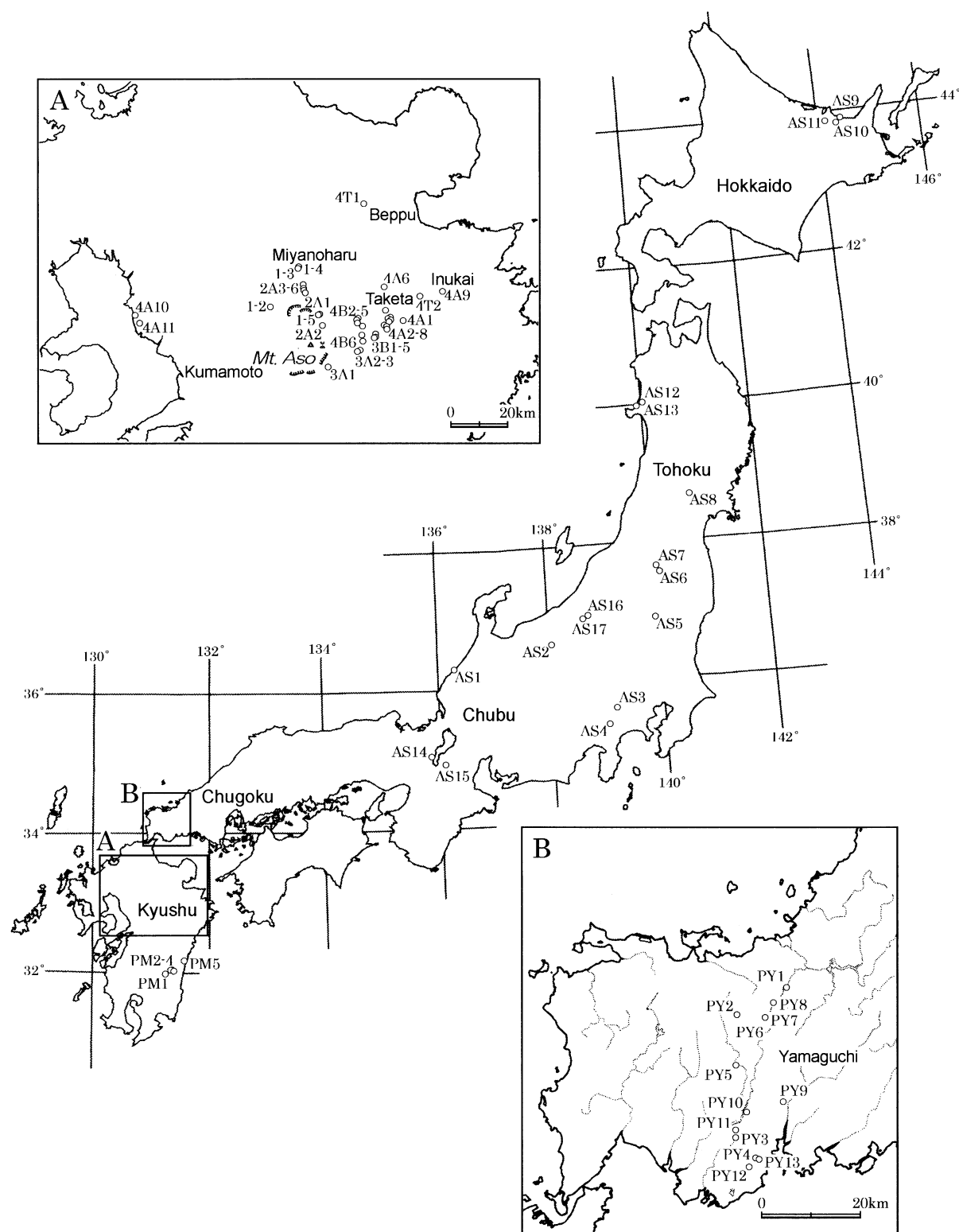
FIGURE 4. Locality map showing paleomagnetic sampling sites. Samples from sites 1-1 to 1-5, 2A1 to 2A6, 3A1 to 3A3, 3B1 to 3B6, 4A1 to 4A11, 4T1 to 4T2, and 4B1 to 4B6 were collected from pyroclastic-flow deposits of Aso-1, Aso-2A, Aso-3A, Aso-3B, Aso-4A, Aso-4T, and Aso-4B, respectively. Samples from sites AS1 to AS17 were collected from the Aso-4 co-ignimbrite ash-fall deposit, and those from sites PM1 to PM5 and PY1 to PY13 were collected from the Aso-4 distal ash-flow deposits in Miyazaki and Yamaguchi Prefectures, respectively.

Kyushu region					Chugoku region
Kitakyushu district (Gohara *et al.*, 1964)	Kumamoto district (Watanabe, 1978)	Miyanoharu district (Kamata, 1997)	Taketa district (Ono *et al.*, 1977)	Beppu and Inukai districts (Hoshizumi *et al.*, 1988; Teraoka *et al.*, 1992)	Yamaguchi Prefecture (Kameyama, 1968)
	Kunomine scoria-flow	Aso-4B (welded tuff)	Aso-4B (welded tuff) ●		
Tosu loam	Tosu orange pumice-flow	Aso-4T (pumice-flow)		Aso-4T (pumice-flow) ●	PYU ●
	Benri scoria-flow Motoigi grey pumice-flow				
Yame clay ●	Yame pumice-flow	Aso-4A (welded tuff)	Aso-4A (welded tuff) ●	Aso-4A (non-welded) ●	PYL ●
	Hatobira pumice-flow Koei ash-flow Oyatsu white pumice-flow				

PYU: Upper part of the Ube volcanic ash
PYL: Lower part of the Ube volcanic ash

FIGURE 5. Stratigraphy of the Aso-4 tephra in the area around Aso caldera. Stippled zones indicate the horizons correlated by stratigraphic studies. A dotted line in the Kumamoto district shows the subunit boundary which is slightly weathered and undulated at many places. Sampled subunits are shown by solid circles.

into three distinctive subunits (Aso-4A, Aso-4T, and Aso-4B) in the area northeast of Aso caldera. Figure 5 shows the stratigraphic relationship of subunits in Aso-4. Paleomagnetic samples were collected from the three horizons correlated to Aso-4A (11 sites: 4A1-11), Aso-4T (2 sites: 4T1-2), and Aso-4B (6 sites: 4B1-6) in central Kyushu. Samples from sites 4A1 to 4A8 and 4B1 to 4B6 are welded tuffs from Aso-4A and Aso-4B, respectively, in the Taketa district. Those from site 4A9, from sites 4A10 to 4A11, and from sites 4T1 to 4T2 are non-welded tuff (Aso-4A) in the Inukai district, clay (the Yame clay) in the Kitakyushu district, and pumice-flow deposit (Aso-4T) in the Beppu district, respectively.

The Aso-4 distal ash-flow deposit in the Chugoku region's Yamaguchi Prefecture is named the Ube volcanic ash layer. The lower and upper parts (PYL and PYU) are correlated to Aso-4A and Aso-4T in the source area, respectively (Gohara et al., 1964; Kameyama, 1968; Watanabe, 1978; Kamata, 1997). Paleomagnetic samples were collected from both PYL (9 sites: PY1L-5L, 8L, 10L-12L) and PYU (11 sites: PY1U-2U, 4U-9U, 11U-13U) of the Ube volcanic ash layer.

Samples from sites PM1 to PM5 were collected from the Aso-4 distal ash-flow deposit in Miyazaki Prefecture. Here the ash-flow deposit (PM) is 20 to 100 cm thick, and is situated within the Hyuga loam (Endo and Suzuki, 1986).

2.3 The Aso-4 co-ignimbrite ash-fall deposit

Machida et al. (1985) discovered a distal ash layer at several localities in Japan with similar petrographic and chemical properties to those of Aso-4, and interpreted it as a co-ignimbrite

ash-fall deposit from the Aso-4 eruption. The ash, named the Aso-4 ash, is a vitric, fine-grained volcanic ash consisting of bubble-walled glass shards, and brown hornblende and orthopyroxene (bronzite) mafic phenocrysts; these characteristics are similar to those of Aso-4. The Aso-4 ash mantles extensive regions from Kyushu to Hokkaido and is also recognized in piston cores from the Sea of Japan and the northwest Pacific Ocean (Machida and Arai, 1992), thus providing a very important datum plane within the late Pleistocene sequence in and around Japan.

The Aso-4 co-ignimbrite ash-fall deposit (AS) was sampled at 17 sites in wide areas from Chubu to Hokkaido. Samples at site AS1 in Ishikawa Prefecture were collected from a 4-cm-thick Aso-4 ash bed in a marine sand deposit (Toyokura et al., 1991). Samples at site AS2 in Nagano Prefecture were collected from a 10-cm-thick ash bed in the lacustrine Takano Formation (Kimura, 1996). Samples at site AS3 in Yamanashi Prefecture were collected from a 10-cm-thick ash bed in a lacustrine deposit (Yonezawa et al., 1996). Samples at site AS4 in Shizuoka Prefecture were collected from a 3-cm-thick ash bed in the fluvial Suruga Conglomerate Member (Machida et al.,1985). Samples at site AS5 in Tochigi Prefecture were collected from a 10-cm-thick ash bed in a fluvial terrace deposit (Suzuki, 1993). Samples at sites AS6 and AS7 in Fukushima Prefecture were collected from 2-cm-thick ash beds in a volcanic soil (Suzuki et al., 1995). Samples at site AS8 in Miyagi Prefecture were collected from a 10-cm-thick ash bed in a lacustrine deposit (Yagi and Soda, 1989). Samples at sites AS9, AS10, and AS11 in the northeast part of Hokkaido were collected from ash beds
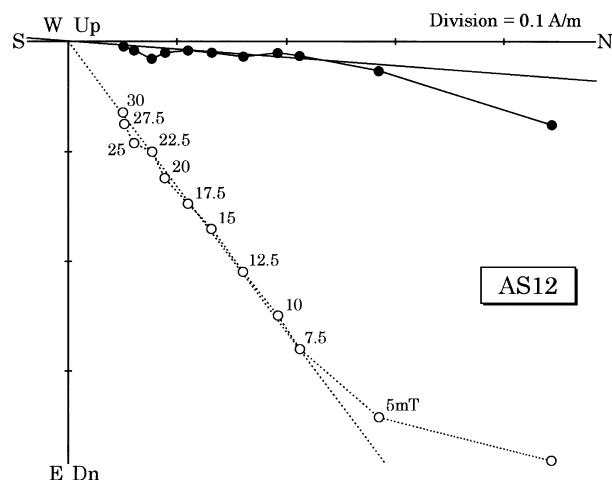
FIGURE 6. Examples of orthogonal plots of AFD data for the Aso-4 co-ignimbrite ash-fall deposit. Solid and open circles represent projection onto horizontal and vertical planes, respectively.

about 15 cm thick. The ash beds at sites AS9 and AS11 are in a sandy gravel; and the ash bed at site AS10 is overlain by the Kutcharo pyroclastic-flow deposit II/III (Okumura, 1991). Samples at sites AS12 and AS13 in Akita Prefecture were collected from ash beds about 5 and 15 cm thick, respectively, in the marine Katanishi Formation (Shiraishi et al., 1992). Samples at sites AS14 and AS15 in Shiga Prefecture were collected from ash beds 4 to 8 cm in thickness within a fluvial terrace deposit (Kimura et al., 1998). Samples at sites AS16 and AS17 in Niigata Prefecture were collected from ash beds 1 to 5 cm in thickness within the Kaisaka Loam Formation (Watanabe and NVARG, 1999).

From the Aso-4 distal ash-flow (PM, PYL, PYU) and co-ignimbrite ash-fall (AS) deposits, twelve to twenty oriented samples were collected at each site using the sampling method of inserting 24 mm plastic cubes into the stratum. At the bottom of the cube, a hole 1 mm in diameter was made for air escape. The sampling apparatus consists of a cylinder-like block with a hole to insert the plastic cube, a piston rod, a board to fix the block, and a magnetic compass (Hirooka, 1988; Nakajima and Fujii, 1995a).

3. PALEOMAGNETIC MEASUREMENTS

Measurements of a specimen's remanent magnetization were made with a flux-gate spinner magnetometer (Natsuhara Giken Co., Model SMM-85). Alternating field demagnetization (AFD) was carried out progressively in more than 5 steps up to 70 mT for all samples with a two-axis tumbler contained in a three-layer mu-metal shield. Magnetic susceptibility of each sample was measured using a susceptibility meter (Bartinton
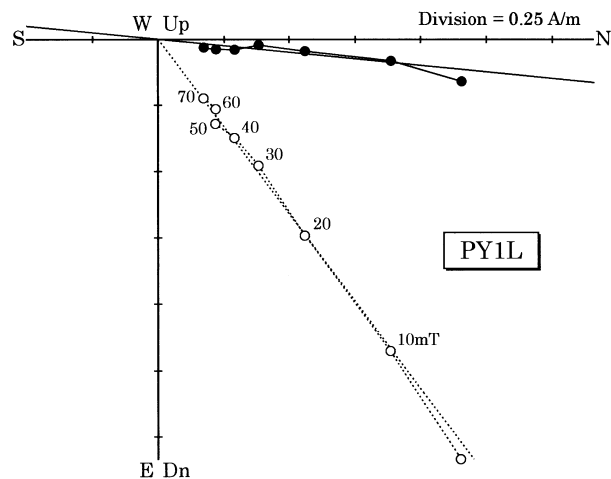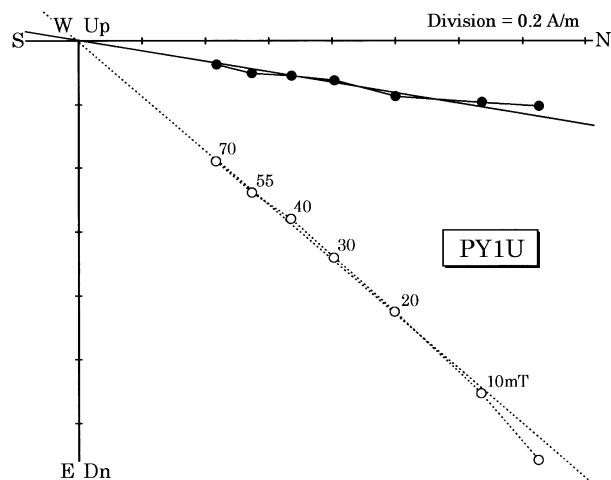

FIGURE 7. Examples of orthogonal plots of AFD data for the Aso-4 distal ash-flow deposit. Solid and open circles represent projection onto horizontal and vertical planes, respectively.

Instruments Ltd., Model MS2B) after AFD.

The AFD experiments on samples of the Aso-4 co-ignimbrite ash-fall (Fig. 6) and distal ash-flow (Fig. 7) deposits show that after removal of a small unstable component by 5 or 10 mT, the characteristic magnetization decayed toward the origin of the orthogonal projection plots. The characteristic magnetizations of welded tuff specimens were also very stable to AFD. The specimen magnetizations at 12 sites (1-2, 1-3, 1-4, 2A3, 2A4, 3B5, 3B6, 4A3, 4A5, 4A6, 4B1, 4B3) decayed linearly toward the origin of the orthogonal projection plots during AFD (Fig. 8A). Although the magnetizations at the other welded tuff sites included unstable components, the unstable components were removed by AFD with peak fields less than 30 mT (Fig. 8B).

Thermal demagnetization (ThD) up to 580°C was carried out

FIGURE 9. Examples of orthogonal plots of ThD data for the Aso-4 welded tuff. Solid and open circles represent projection onto horizontal and vertical planes, respectively.
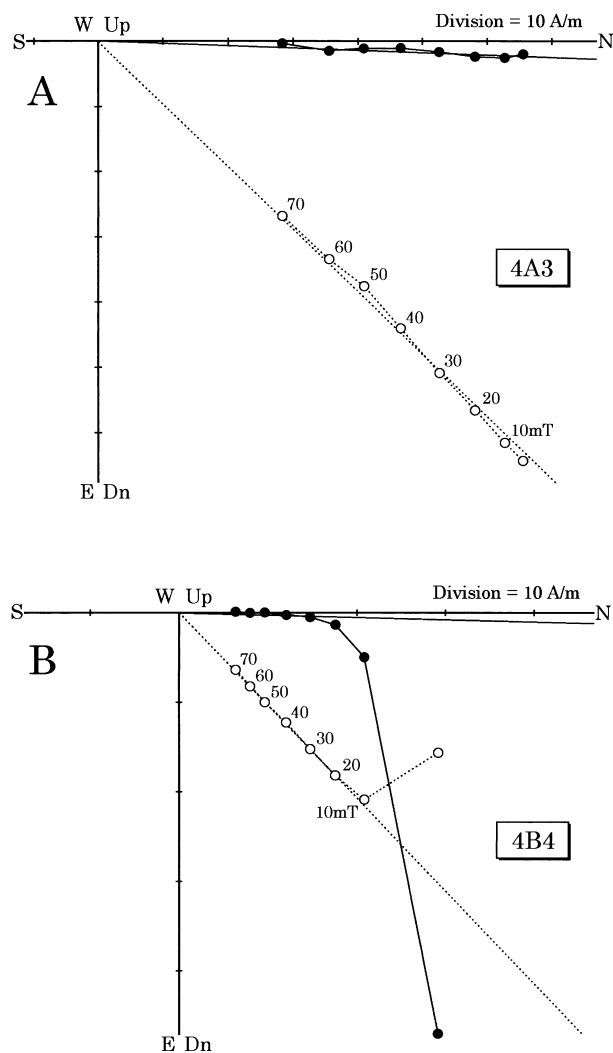

FIGURE 8. Examples of orthogonal plots of AFD data for the Aso-4 welded tuff. Solid and open circles represent projection onto horizontal and vertical planes, respectively.

progressively in 7 steps on three pilot specimens from each welded tuff site. The Aso-4 co-ignimbrite ash-fall and distal ash-flow samples could not be subjected to ThD, because they were held in plastic cubes with a melting temperature of 160°C. The specimens were heated in air using a noninductively wound electric furnace. The stray field during the cooling cycle was reduced to less than 10 nT using a cylindrical three-layer mu-metal shield. The ThD instrument and thermo-controller (Model DEM-8602) were provided by Natsuhara Giken. In order to check thermal alteration of the magnetic minerals, susceptibility measurements of the specimens were made at each demagnetization level.

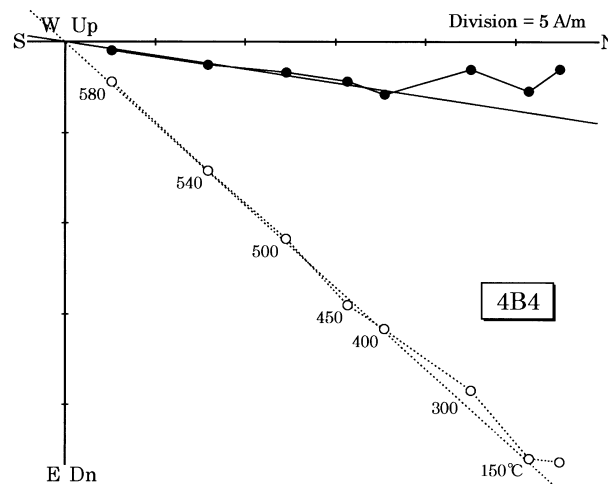Unstable components were removed by demagnetization at temperatures lower than 400°C (Fig. 9). Rapid decreases in the magnetic intensity were observed at low temperature levels for specimens at five sites: 1-5, 4A1, 4A2, 4A3, and 4A8 (Fig. 10). The rapid decreases likely indicate the presence of secondary magnetic minerals such as goethite and pyrrhotite. The characteristic directions of these specimens, however, were considered to be the primary magnetizations because these directions are the same as those obtained from other specimens without the rapid intensity decrease at low temperatures. At the other sites, the specimens had high blocking temperatures, and their magnetizations were mostly removed by ThD up to 580°C. These evidences suggest that the magnetic minerals carrying the characteristic magnetization are mainly magnetites or titanomagnetites with low titanium content. Since the change in susceptibility at each demagnetization level was less than 10 % of the value before demagnetization, the alteration of the magnetic minerals by heating is presumed to be minor.

Directions of the primary magnetic components were computed using principal component analysis (Kirschvink, 1980); three-dimensional least-squares fits were made of the demagnetization data after removing unstable components with the line forced to include the origin (anchored). Site-mean directions were calculated using the AFD data because the same primary magnetic component was detected by both demagnetization methods (Fig. 11).

Results of paleomagnetic measurements are shown in Table 2. The ash samples were collected only from horizontal strata. Eutaxitic structures of flattened obsidian lenses in the welded tuffs are mostly horizontal, and there is no evidence of significant tilting of strata. Therefore, no tilt correction was made to the magnetic directions in Table 2. The unit- and subunit-means for the Aso-1 to Aso-4 welded tuffs and the
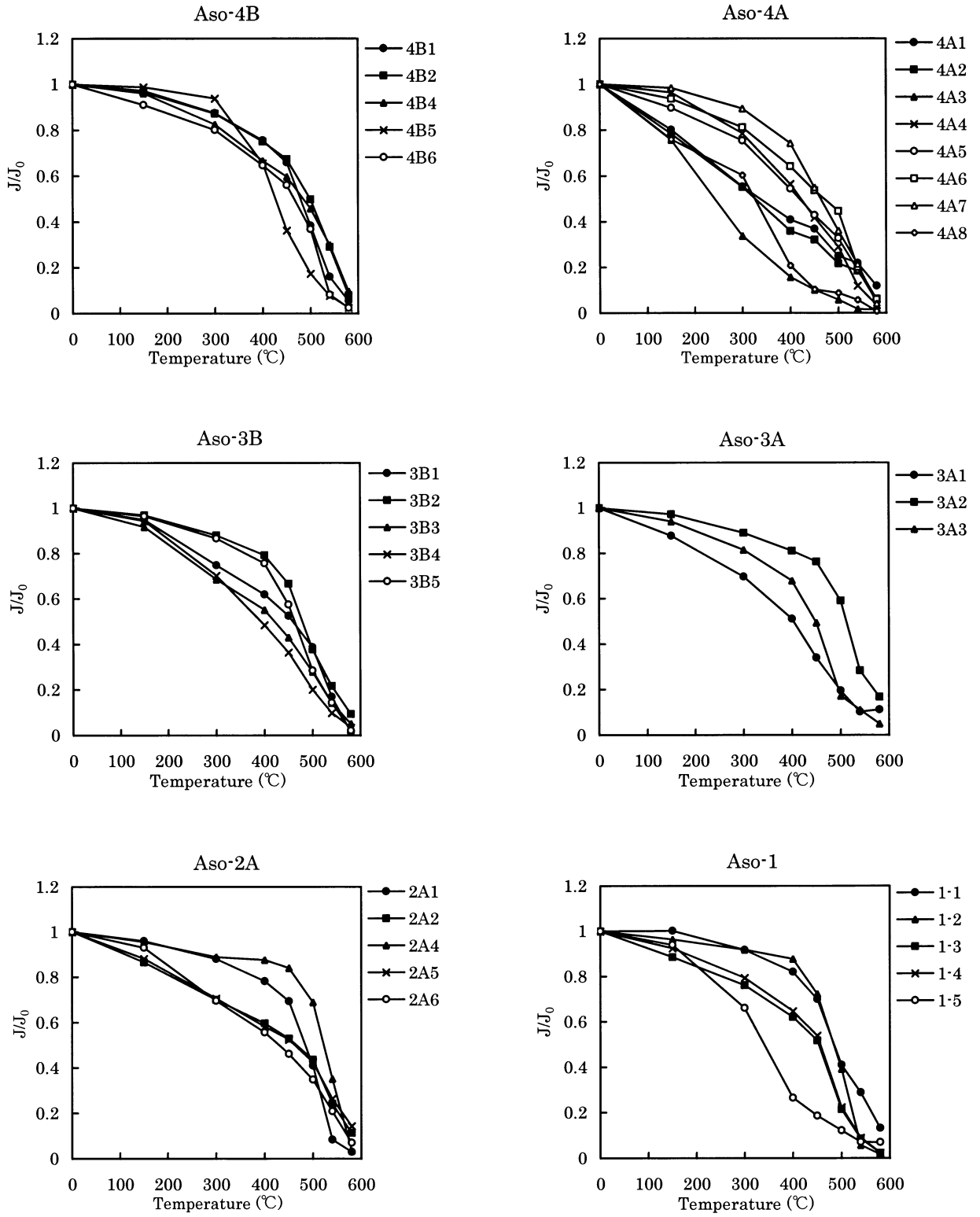
FIGURE 10. ThD curves where relative intensity is plotted against demagnetizing temperature.

4. IRM ACQUISITION AND THD OF A THREE-COMPONENT IRM

Magnetic minerals contained in the welded tuff specimens are likely to be magnetites or titanomagnetites on the basis of the ThD results. Since ThD experiments were not performed on the ash samples, it is not certain what magnetic minerals are in the ash samples. Progressive acquisition of isothermal remanent magnetization (IRM) and ThD of a three-component IRM (Lowrie, 1990), therefore, were investigated to identify the ferromagnetic mineral content in the ash samples.

For the IRM experiments, one sample from each site was arbitrarily chosen after AFD. Because they are unconsolidated and readily disintegrate, the ash samples were held in plastic cubes, which melt at about 160°C. Synthetic specimens were prepared using the ash samples and plaster of Paris for ThD of the induced IRM.

The IRM acquisition experiments were carried out using a pulse magnetizer (Magnetic Measurements Ltd., Model MMPM10) in magnetic fields with intensities up to 3 T. A three-component IRM was produced by applying a different DC field (3, 0.4, and 0.12 T) to each of the three perpendicular axes of the specimen with the pulse magnetizer. The acquisition and ThD curves of the IRM components for all specimens show similar features. The smooth IRM acquisition curves rise steeply up to 100 mT, and reach saturation by 400 mT (Fig. 13). The ThD of each IRM component is plotted separately in Fig. 14. The ThD curves show that the soft (<0.12 T) coercivity fraction is the largest, and that the medium (0.12 to 0.4 T) and hard (0.4 to 3 T) fractions are minor. The soft coercivity fraction was demagnetized smoothly to zero by 580°C, indicating that the specimens' magnetic mineralogy is also dominated by magnetites and titanomagnetites.

5. PALEOMAGNETIC DIRECTIONS

5.1 Welded tuffs of the Aso pyroclastic-flow deposits

Magnetic directions of welded tuffs are grouped tightly for each unit or subunit, and are all of normal polarity (Fig. 15). Unit-mean (Aso-1, Aso-2, Aso-3, and Aso-4) and subunit-mean (Aso-3A, Aso-3B, Aso-4A, and Aso-4B) directions are shown in Table 3. Figure 16 shows the unit-mean directions plotted on an equal area net. The curve in Fig. 16 is the standard geomagnetic secular variation (GSV) curve for southwestern Japan determined by Hirooka (1977) for the past 2,000 years. The unit-mean directions of Aso-1 and Aso-4 are near the GSV curve and the present geomagnetic field direction (D = –6°, I = 46°). The unit-mean directions of Aso-2 and Aso-3, however, are far away from the recent GSV curve. The inclination of Aso-2 is unusually steep, and the declination of Aso-3 is more easterly. It appears that the distinctive directions of Aso-2 and Aso-3 could be useful in identifying these tephras. The steep inclination of Aso-2 has also been pointed out by Shibuya et al.
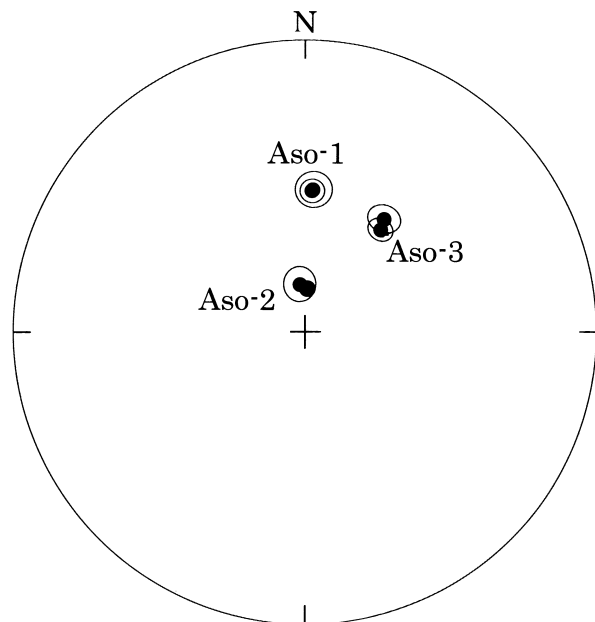

FIGURE 11. Unit-mean directions after AFD and after ThD for Aso-1, Aso-2, and Aso-3. Significant differences are not observed between the two directions for each unit.

Aso-4 tephra are tabulated in Tables 3 and 4, respectively.

Subunit-mean susceptibilities of proximal welded tuff samples from Aso-1, Aso-2A, Aso-3A, Aso-3B, and Aso-4B are distributed in a comparatively narrow range between 7.7 and 10.9 μm³/kg (Fig. 12). Subunit-mean susceptibility of Aso-4A is smaller than that of Aso-4B. Subunit-mean susceptibilities of distal ash-flow samples from PM, PYL, and PYU are similar to the value of proximal welded tuff samples from Aso-4A. Site-mean susceptibilities of the Aso-4 co-ignimbrite ash-fall samples are distributed in a wide range between 0.2 and 10.4 μm³/kg. Samples with susceptibilities smaller than 0.5 μm³/kg were taken mainly from Tohoku and Hokkaido far away from Aso caldera. The regional difference in susceptibilities, therefore, is likely related to the decreasing amount of ferromagnetic minerals in the Aso-4 co-ignimbrite ash-fall samples with increasing distance from the source volcano, as were demonstrated in the Pleistocene Azuki co-ignimbrite ash (Kamata et al., 1997) and AT (Nakajima and Fujii, 1995b).

Intensities of magnetization for welded tuff specimens are on the order of 10^{-3} Am²/kg, and ash samples on the order of 10^{-5} to 10^{-4} Am²/kg. In addition, mean destructive fields for the proximal welded tuffs (40 to 50 mT) are higher than those for the Aso-4 co-ignimbrite ash-fall and distal ash-flow samples by about 30 mT.

TABLE 2. Paleomagnetic results from the Aso pyroclastic-flow and the Aso-4 co-ignimbrite ash-fall deposits. N: number of specimens, Dm and Im: site-mean declination and inclination, α_{95} and k: radius of 95% confidence circle and Fisher's precision parameter (Fisher, 1953), VGP: virtual geomagnetic pole position, MDF: median destructive field, INT: intensity of remanent magnetization before demagnetization.

Site	Locality	N	Dm (°E)	Im (°)	α_{95} (°)	k	VGP Lon. (°E)	VGP Lat. (°N)	MDF (mT)	INT (10^{-3}Am^2/kg)	Susceptibility (μ m^3/kg)
Welded tuff											
Aso-4B											
4B1	Sakuramachi	10	-1.3	40.2	3.1	238.5	318.2	79.9	60	4.87	8.10
4B2	Ikebe-1	10	-9.3	37.9	3.8	159.8	348.8	75.7	26	6.32	11.17
4B3	Amakunugi	10	-9.9	32.1	1.6	909.0	343.5	72.1	65	6.00	14.96
4B4	Shindo	10	-1.6	43.5	4.2	136.0	322.1	82.3	30	4.67	10.72
4B5	Ikebe-2	10	0.6	37.9	2.0	572.2	308.5	78.3	50	5.10	11.27
4B6	Miyabira	8	-9.1	41.6	2.0	790.9	355.3	78.0	15	1.46	6.27
Aso-4A											
4A1	Harajiri	11	-6.2	47.3	3.1	223.6	2.8	83.0	33	0.09	2.63
4A2	Namese	10	-4.6	47.8	3.7	170.3	356.6	84.3	29	0.86	3.99
4A3	Madokoro	10	-1.0	43.5	2.7	322.6	318.2	82.3	>70	1.80	3.34
4A4	Shichiri	11	-4.2	44.7	2.0	506.3	341.3	82.4	31	1.84	10.82
4A5	Taketa 1	9	-8.0	42.8	2.4	471.8	354.2	79.3	32	1.06	8.98
4A6	Yunoharu	8	-5.7	39.3	3.2	304.8	337.8	78.1	>70	1.10	8.38
4A7	Taketa 2	10	-7.6	44.7	3.1	246.3	358.2	80.6	35	1.56	9.94
4A8	Uetsuno	10	-5.0	44.4	3.1	248.6	345.0	81.9	20	0.05	1.51
Aso-3B											
3B1	Deai 1	10	38.1	44.3	3.1	250.9	223.0	56.3	32	2.77	8.48
3B2	Deai 2	10	40.8	47.5	3.5	186.6	217.2	54.9	>70	5.87	9.49
3B3	Shichiri	9	37.4	54.5	2.5	420.5	207.0	59.1	35	0.78	5.71
3B4	Nakao	8	29.2	56.1	2.4	525.5	204.3	65.8	35	1.27	6.30
3B5	Sarukuchi	7	30.3	49.8	3.0	412.8	218.3	64.2	65	2.62	6.82
3B6	Ibuse	9	35.7	50.9	3.4	224.4	214.0	59.9	50	4.52	9.48
Aso-3A											
3A1	Yanagidani	9	34.6	57.5	2.6	401.1	200.6	61.5	52	2.28	5.67
3A2	Nagano	10	29.0	48.8	3.8	159.8	220.7	65.1	38	2.95	8.82
3A3	Futamata	10	44.3	48.3	3.2	224.2	214.6	52.2	60	3.35	9.00
Aso-2A											
2A1	Shiroyama	9	-9.9	75.0	2.5	422.0	121.7	60.5	60	4.02	8.07
2A2	Takimurozaka	10	3.1	70.1	2.8	294.2	136.2	68.7	40	2.44	13.51
2A3	Kikawa 1	3	-47.1	79.6	5.5	496.3	110.1	45.1	38	3.87	10.94
2A4	Kikawa 2	9	-11.2	76.2	3.7	193.4	121.7	58.4	>70	3.61	6.67
2A5	Takinokuchi	10	9.1	74.3	3.3	220.7	140.5	61.8	45	7.20	20.39
2A6	Tonashi	10	0.2	79.6	2.1	530.0	131.2	53.2	32	0.95	5.77
Aso-1											
1-1	Taketa	8	9.6	46.8	4.6	147.2	249.7	80.4	60	3.13	12.24
1-2	Kikuchi-keikoku	12	-2.0	42.7	4.0	119.7	323.5	81.6	50	8.39	9.64
1-3	Shinbashi 1	10	3.1	49.7	2.1	513.5	264.8	86.3	40	2.82	9.28
1-4	Shinbashi 2	8	1.9	50.2	2.3	588.9	273.8	87.3	40	2.81	8.92
1-5	Shiroyama	7	5.1	55.4	4.5	182.9	184.6	84.9	50	3.03	7.13

TABLE 2. (continued)

Site	Locality	N	Dm (°E)	Im (°)	α_{95} (°)	k	VGP Lon. (°E)	VGP Lat. (°N)	MDF (mT)	INT (10^{-5}Am^2/kg)	Susceptibility (μ m^3/kg)
Aso-4T pumice-flow deposit											
4T1	Hijyudai	16	-5.4	42.2	1.5	515.1	340.6	79.9	30	33.20	5.74
4T2	Taniinuyama	11	-6.5	42.8	1.4	1119.1	347.9	80.0	10	31.80	10.20
Aso-4A pyroclastic-flow deposit (non-welded)											
4A9	Osako	13	-7.5	46.5	2.5	283.4	4.4	81.7	28	124.00	10.74
Yame clay											
4A10	Nakamasunaga	15	1.1	46.8	1.9	402.5	299.3	85.0	11	2.06	0.58
4A11	Takahama	15	-7.9	44.8	3.3	137.9	359.3	80.6	8	0.52	0.17
Aso-4 distal ash-flow deposit											
(Yamaguchi Prefecture)											
PY1U	Sumouba	20	-1.7	40.8	1.5	472.8	319.5	78.9	25	15.15	3.18
PY1L		12	-2.5	49.7	3.6	146.1	341.1	85.7	20	17.51	4.13
PY2U	Shibao	24	1.6	44.4	1.6	341.0	301.3	81.7	15	33.75	3.93
PY2L		9	2.1	46.1	3.0	284.8	295.9	82.9	5	16.10	5.42
PY3L	Tanoono	12	2.0	42.5	1.9	532.3	300.3	80.4	23	37.80	9.69
PY4U	Oka	28	-0.1	41.1	1.5	344.7	311.8	79.6	20	27.56	5.85
PY4L		12	-4.0	48.6	3.0	216.5	349.8	84.4	19	29.00	7.90
PY5U	Iwanagaichi	27	-6.9	44.1	1.6	286.6	348.7	79.8	23	14.03	4.69
PY5L		19	-8.2	45.5	2.2	244.0	357.8	79.9	13	12.56	5.28
PY6U	Ogawa	12	-3.0	45.7	2.1	411.0	332.0	82.4	13	9.31	4.97
PY7U	Matsubara	11	0.4	51.7	1.8	667.6	301.4	88.0	26	32.89	5.71
PY8U	Nitanda	12	-0.6	43.5	2.9	226.1	314.9	81.1	11	5.00	5.00
PY8L		11	-0.8	46.9	2.5	339.9	317.9	83.8	11	0.41	0.35
PY9U	Shinmachihigashikami	9	3.4	34.1	6.0	74.8	299.4	74.4	5	80.93	11.66
PY10L	Hanaga	7	-0.2	50.0	3.6	275.6	314.3	86.7	12	10.21	7.28
PY11U	Arase	12	-3.1	35.8	2.2	404.8	323.0	75.5	21	19.17	5.13
PY11L		8	2.5	42.9	2.9	377.7	297.3	80.6	20	35.80	6.19
PY12U	Senzai	12	4.4	46.2	2.0	508.1	279.8	82.5	28	18.98	5.74
PY12L		10	-6.9	49.5	3.9	158.1	11.2	83.1	12	5.50	5.59
PY13U	Hamaomote	10	-5.3	49.8	4.0	145.6	5.7	84.4	9	4.44	4.53
(Miyazaki Prefecture)											
PM1	Kunitomi	16	0.2	48.0	2.0	345.3	308.0	87.0	6	32.30	7.10
PM2	Tonokoori 1	16	1.7	45.1	5.1	53.7	295.6	84.4	5	9.07	7.25
PM3	Tonokoori 2	15	1.0	39.5	2.9	179.5	305.9	80.3	6	2.27	1.39
PM4	Chugenbaru	15	-3.5	51.1	1.5	676.2	37.3	87.0	20	33.80	4.92
PM5	Heda	17	-2.0	39.9	1.7	459.4	322.6	80.3	10	1.48	0.73
Aso-4 co-ignimbrite ash-fall deposit											
AS1	Kurosaki	14	-3.6	50.3	1.9	419.7	346.9	83.9	6	3.22	2.47
AS2	Takano	17	6.0	51.8	1.7	445.5	266.1	83.6	10	5.94	2.31
AS3	Uenohara	16	-2.0	51.1	1.7	466.0	343.2	85.8	13	17.20	4.21
AS4	Oyama	23	4.9	43.5	1.6	352.6	294.8	79.2	14	20.60	6.01
AS5	Nishinasuno	17	4.8	53.3	2.4	231.4	266.5	85.0	8	9.03	6.03
AS6	Hayama	13	-15.9	48.2	4.7	78.5	22.5	74.4	20	16.10	4.10
AS7	Hibara-ko	8	-2.7	52.3	5.9	90.3	345.7	84.8	3	9.21	10.39
AS8	Naruko	13	-8.5	47.2	3.6	135.3	357.3	77.4	25	1.03	0.18
AS9	Koshimizu	23	-3.5	56.8	2.5	145.2	347.8	83.0	15	0.75	0.18
AS10	Abashiri	22	0.9	55.2	4.4	51.2	319.2	81.9	16	2.47	0.39
AS11	Memanbetsu	13	-1.0	61.6	4.0	106.1	357.6	88.7	18	1.75	0.24
AS12	Asanai	13	-2.2	50.6	2.4	305.4	332.1	81.0	11	5.39	2.50
AS13	Yasuda	17	0.6	53.0	7.0	26.7	315.4	83.6	9	0.72	0.27
AS14	Ikadachi	21	0.3	53.1	2.3	197.6	306.3	88.5	10	2.76	2.73
AS15	Shigaraki	16	1.1	48.9	1.5	623.4	305.4	84.8	4	1.98	0.56
AS16	Miho	12	-9.0	58.3	2.7	251.0	67.3	82.6	12	8.34	5.40
AS17	Oyachi	7	-10.6	51.2	4.4	189.0	21.6	79.9	6	10.12	4.70

FIGURE 12. Susceptibilities versus NRM's intensities plotted on logarithmic scales. Solid squares show subunit-means for welded tuffs of the Aso pyroclastic-flow deposits (Aso-1, Aso-2A, Aso-3A, Aso-3B, Aso-4A, and Aso-4B), the Aso-4 distal ash-flow deposits (PYL, PYU, and PM), and the Aso-4 co-ignimbrite ash-fall deposit (AS), and solid circles show site-means for AS. Error bars are standard deviations.

FIGURE 13. Progressive acquisition of IRM in an ash sample.

FIGURE 14. Example of ThD of a three-component IRM produced by applying different DC fields (3, 0.4, and 0.12 T) to each of the three perpendicular sample axes.

(1999). When the magnetic directions are compared between the subunits, the inclination of Aso-4A is steeper than that of Aso-4B by 5°, although such a difference is not seen between directions for the subunits of Aso-3: Aso-3A and Aso-3B (Fig. 17).

Since geomagnetic excursions and short-term geomagnetic events between the Aso-1 (266 ka) and the Aso-4 (89 ka) eruptions have been reported in previous paleomagnetic studies (Kawai et al., 1971; Hyodo et al., 1993; Hyodo and Minemoto, 1996; Hyodo, 1999), it was expected that geomagnetic events like the Blake and the Biwa II events would be recorded by these welded tuffs. However, no directions indicating geomagnetic excursions or short events with reversed polarity were found in the welded tuffs.

5.2 The Aso-4 tephra

The Aso-4 tephra consists of proximal pyroclastic-flow deposits (Aso-4A, Yame clay, Aso-4T, and Aso-4B), distal ash-flow deposits (PM, PYL, and PYU), and co-ignimbrite ash-fall deposit (AS). The sampled subunits of Aso-4 in the area around the source caldera are divided into three stratigraphic groups: 4A (Aso-4A, Yame clay, and PYL), 4T (Aso-4T and PYU), and 4B (Aso-4B), as shown in Fig. 5. Stratigraphic correlations of AS and PM with the subunits in the source area were not established in previous studies.

The 'geographically corrected site-mean directions' (corrected directions) cluster tightly in each stratigraphic group (Fig. 18). It supports that the stratigraphic correlation within each group is appropriate. The corrected directions are calculated from their virtual geomagnetic poles (VGPs) at a reference point in Aso caldera (131°E, 33°N). The group-mean VGP of 4A is identical to the subunit-mean VGPs of AS and PM (Table 4). To emphasize the difference between other groups, group-mean corrected directions of 4A, 4T, and 4B and subunit-mean corrected directions of AS and PM are shown in Fig. 19. The corrected directions of 4A, AS, and PM are identical to one another with overlapping 95% confidence circles (Fig. 19A). The agreement of the corrected directions indicates that AS and PM were deposited at approximately the same time as 4A. This correlation with the co-ignimbrite ash-fall deposit (AS) is consistent with the fact that 4A covers an extensive area, and is supposed to be the product of the culminate phase of the Aso-4 eruption (Watanabe, 1978).

In the area around the source caldera, the group-mean corrected inclination of 4A is 6.7° steeper than that of 4B, and is 3.8° steeper than that of 4T (Fig. 19B). These inclination differences, in which the lower one is steeper than the upper, were observed at the sites collected from both 4A and 4T in Yamaguchi Prefecture (PY1-2, 4-5, 8, 11-12). In addition, the inclination differences between 4A and 4B were also observed in the limited area of the Taketa district. If the inclination differences were significant, it may be assumed that the differences observed in Yamaguchi Prefecture and the Taketa

district originated from the stratigraphic time gaps rather than from local geomagnetic anomalies.

The group-mean corrected directions of 4A and 4B are distinct at the 5% significance level, because their α_{95} circles do not overlap (Fig. 19B). The group-mean corrected directions of 4A and 4T are not contained within the α_{95} circle of the other group-mean, but the circles overlap only a little. Then the F-test of Watson (1956) is used to determine whether the two directions are distinguishable at the 5% significance level. In this test, the null hypothesis is that the two directional data sets are samples of the same population, and that the difference between the two means is due to sampling errors. The observed F statistic (6.05) exceeds the tabulated value (3.15) for 2 and 62 degrees of freedom at the 5% significance level. Therefore, it is interpreted that these two mean directions of 4A and 4T are different at the 5% significance level. On the other hand, the group-mean corrected direction of 4B is not distinguishable from that of 4T, because the group-mean corrected direction of 4T falls within the α_{95} circle of 4B. Watanabe (1978) reported that the surface of the subunit (the Benri scoria-flow deposit) directly under 4T (the Tosu orange pumice-flow deposit) was slightly weathered and undulated in many places, although paleo-soil, humus and a notable erosional hiatus were not found at the boundaries between the other sequential subunits in the Kumamoto district (Fig. 5). This observation suggests that the time interval between 4A and 4B (or 4T) was longer than that between 4T and 4B. According the above facts, it can be supposed that the directional difference between 4A and 4B (or 4T) in the area around the source caldera originated from ancient GSV.

The difference in eruption times between 4A and 4B can be estimated on the basis of the standard GSV curve (Hirooka, 1977), assuming the inclination difference (6.7°) was caused by GSV. The declinations of both groups are nearly the same. The age when the inclination changed the most, according to the standard GSV curve, is in the 6th century when the inclination changed by about 6° for the period from 550 to 600 A.D. The difference in time between the eruption of 4A and 4B, therefore, can be estimated at 50 years or more.

Nakajima and Fujii (1995a), Hayashida et al. (1996), and Reynolds (1979) showed that ash-fall deposits in areas distal to the source caldera have DRM directions identical to the TRM directions in welded tuffs nearby the source caldera. This observation indicates nearly simultaneous acquisition of TRM and DRM in correlative units. In this study, the corrected directions of co-ignimbrite ash-fall (AS) and distal ash-flow (PM, PYL) samples are also identical to those of proximal welded tuff samples (Aso-4A) in the Aso-4 tephra. It is therefore likely that DRMs of the ash samples are as reliable as TRMs in the welded tuff samples, and that the DRMs and TRMs represent the geomagnetic field direction at the time of the Aso-4A eruption.

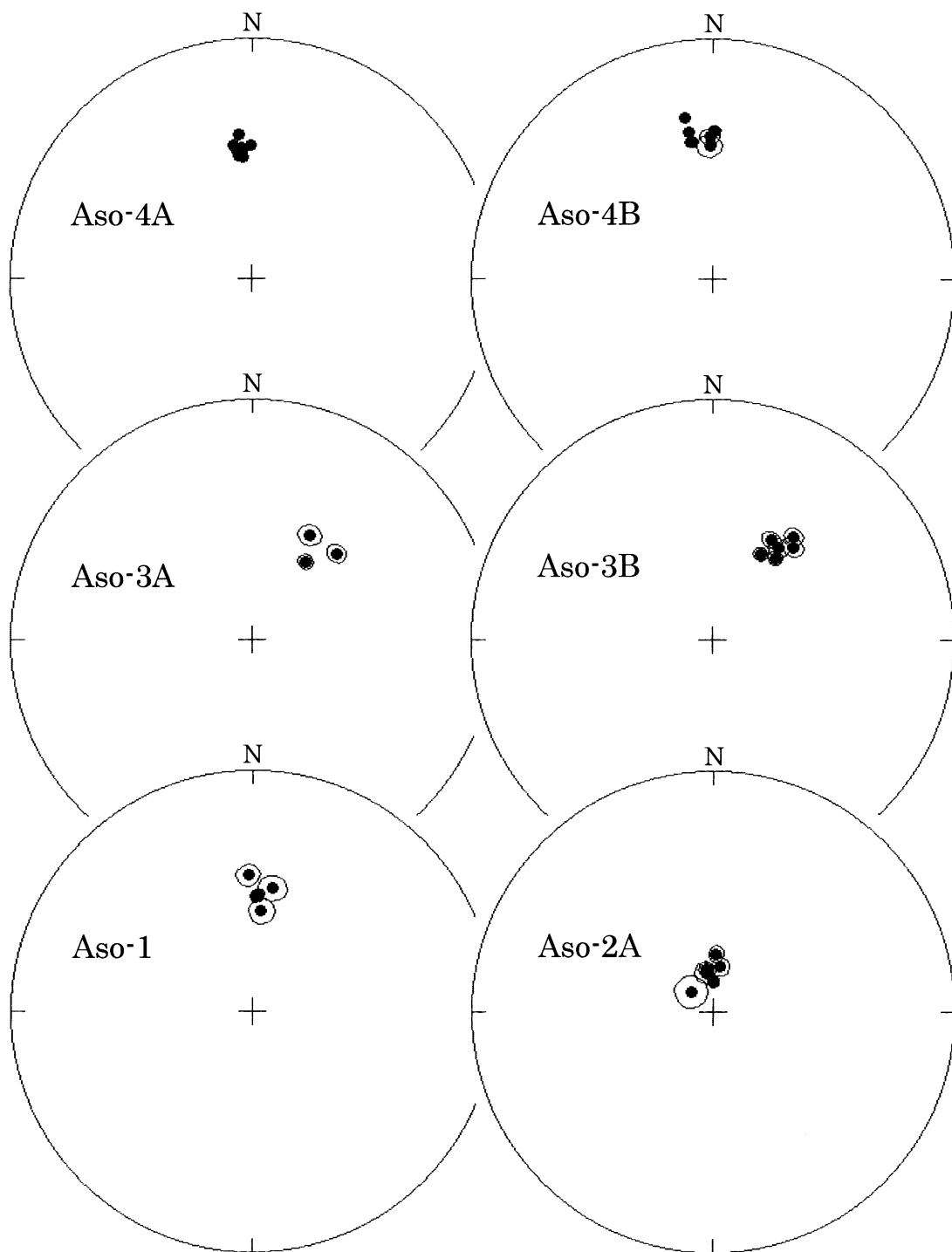Samples from sites AS1 to AS4, AS8, AS9, AS11, and AS13

FIGURE 15. Equal-area projection showing site-mean directions and 95% confidence circles (lower hemisphere) for welded tuffs of the Aso pyroclastic-flow deposit.
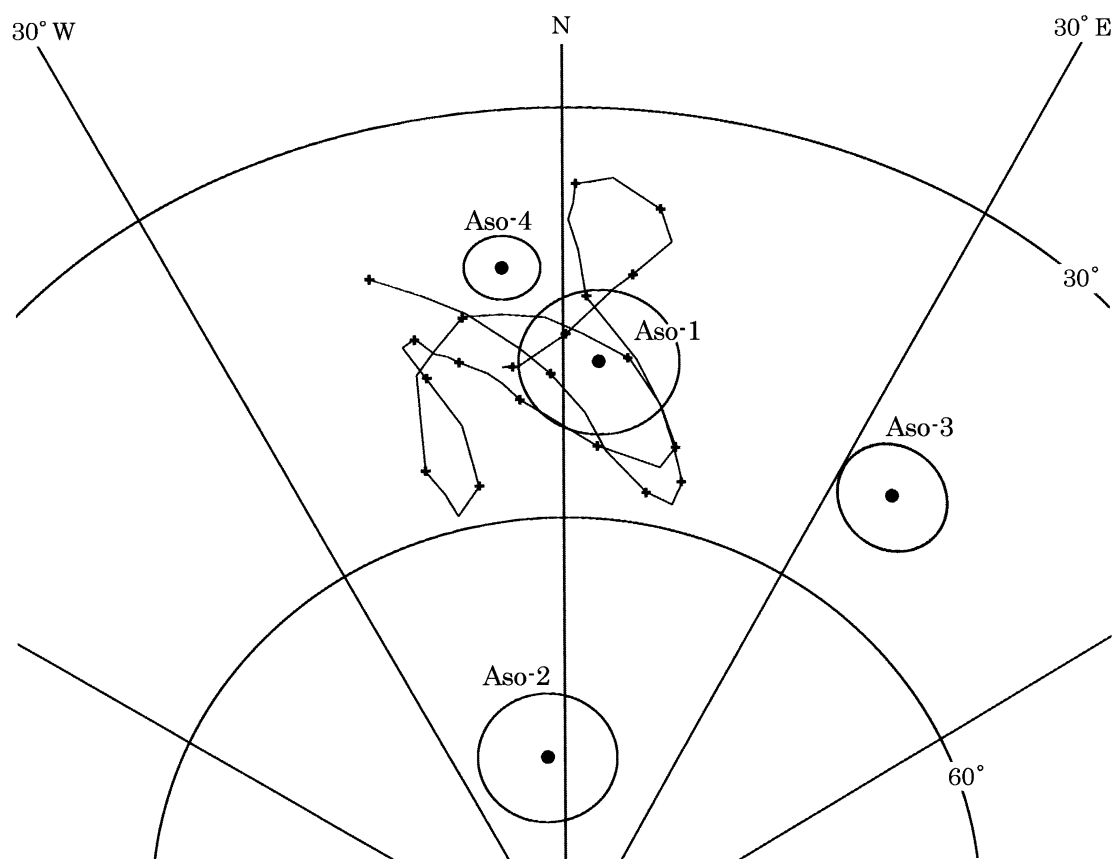
FIGURE 16. Equal-area projection showing unit-mean directions and circles of 95% confidence (lower hemisphere) for welded tuffs of the Aso pyroclastic-flow deposits. The curve shows recent geomagnetic secular variation in southwest Japan. after Hirooka (1977).

were collected from water-laid beds, and those of remaining sites in AS were from aeolian beds. Significant differences between the mean corrected directions of the water-laid and aeolian beds in AS were not detected. The mean corrected directions (N, Dm, Im, α_{95}, k) are (8, –1.8°, 45.9°, 3.4°, 264.1) and (9, –4.3°, 47.7°, 3.8°, 188.2), respectively. Nakajima and Fujii (1995a) also reported that a significant difference was not recognized between the paleomagnetic directions of water-laid and aeolian beds of AT. Both water-laid and aeolian beds of the fine-grained ashes are thought to have acquired stable DRMs at approximately the same time as emplacement of the proximal pyroclastic flow.

6. GEOMAGNETIC FIELD OVER THE JAPANESE ISLANDS AT THE TIME OF THE ASO-4A ERUPTION

Aso-4A, PM, PYL, and AS have identical VGPs (or corrected directions), and were thought to be deposited at the same time. The pyroclastic-flow (Aso-4A) and ash-flow (PM, PYL) deposits are found within 160 km distance from Aso caldera, and the co-ignimbrite ash-fall deposit (AS) is found 500 to 1,600 km from Aso caldera. Figure 20 shows the relation between regional-mean directions and latitudes, which are calculated for central Kyushu (4A1-11), southern Kyushu (PM1-5), Chugoku (PY1L-5L, 8L, 10L-12L), Chubu (AS1-4, 14, 15), Tohoku (AS5-8, 12, 13, 16, 17), and Hokkaido (AS9-11). The obtained regional-mean directions are almost the same as the expected directions. This fact and the identical VGPs in the regions lead us to believe that these remanent magnetizations were acquired under the same geocentric dipole field coeval with the Aso-4A eruption.

In order to clarify the configuration of the geomagnetic field at the time of the AT eruption, Nakajima and Fujii (1995a) used the following procedures. (1) The pole of the geomagnetic
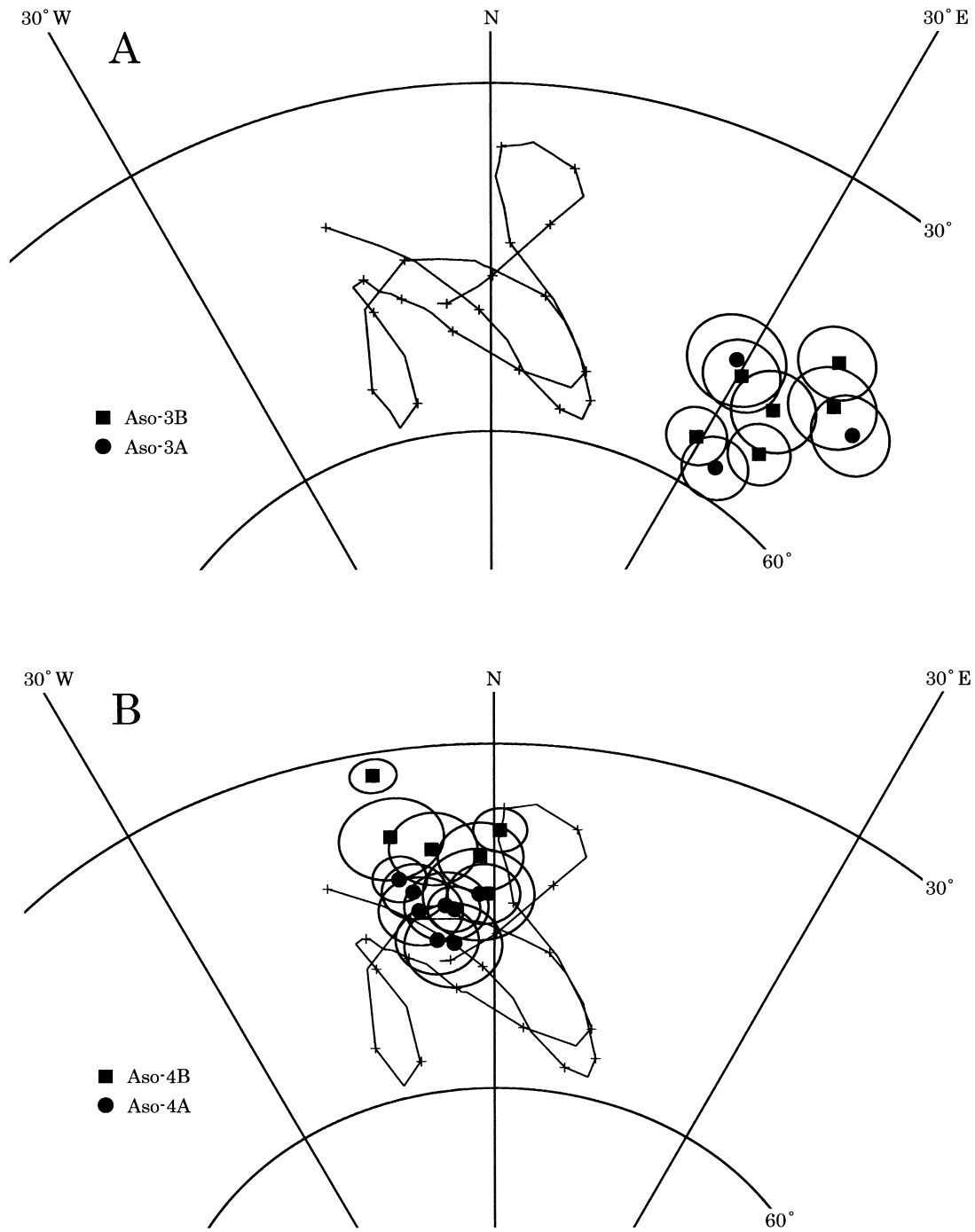
FIGURE 17. Equal-area projection showing site-mean directions and circles of 95% confidence (lower hemisphere) for welded tuffs of Aso-3 (**A**) and Aso-4 (**B**). The curve shows recent geomagnetic secular variation in southwest Japan. after Hirooka (1977).

TABLE 3. Summary of paleomagnetic results for welded tuff samples from the four major units of the Aso pyroclastic-flow deposit. N: number of site-mean data, Dm and Im: unit (or subunit)-mean declination and inclination, and the other notations are the same as those used in Table 2.

Unit	Subunit	N	Dm (°)	Im (°)	α_{95} (°)	k	VGP Lon. (°E)	VGP Lat. (°N)	MDF (mT)	INT (10^{-3} Am^2/kg)	Susceptibility (μm^3/kg)
	Aso-4B	6	-5.2	39.0	4.5	220.3	335.3	78.2	41	4.74	10.4
	Aso-4A	8	-5.3	44.3	2.1	686.7	346.5	81.7	40	1.05	6.20
Aso-4		14	-5.2	42.0	2.4	271.0	340.7	80.3	40	2.63	8.01
	Aso-3B	6	35.4	50.6	4.3	239.7	214.4	60.2	48	2.97	7.71
	Aso-3A	3	36.1	51.7	10.9	128.0	211.9	59.9	50	2.86	7.83
Aso-3		9	35.7	51.0	3.5	216.7	213.5	60.1	49	2.93	7.75
Aso-2	Aso-2A	6	-6.6	76.4	4.7	204.9	123.5	58.7	48	2.68	10.9
Aso-1		5	3.4	49.0	5.2	217.6	265.0	85.8	48	4.04	9.44

TABLE 4. Summary of paleomagnetic results for the Aso-4 tephra. The notations are the same as those used in Tables 2 and 3.

Group	Subunit		N	Dm (°)	Im (°)	α_{95} (°)	k	VGP Lon. (°E)	VGP Lat. (°N)	MDF (mT)	INT (10^{-4} Am^2/kg)	Susceptibility (μm^3/kg)
4B	Aso-4B welded tuff	(Aso-4B)	6	-5.2	39.0	4.5	220.3	335.3	78.2	41	47	10.4
4T			13					321.6	81.3			
	Aso-4T pumice-flow deposit	(Aso-4T)	2							20	0.33	7.97
	Aso-4 distal ash-flow deposit (Yamaguchi Pref.)	(PYU)	11	-0.9	43.4	3.3	191.3	317.2	81.3	18	2.4	5.49
4A			20						338.9	83.0			
	Aso-4A pyroclastic-flow deposit*	(Aso-4A)	11	-5.2	44.8	1.8	649.3	347.1	82.1	33	8.8	5.55
	Aso-4 distal ash-flow deposit (Yamaguchi Pref.)	(PYL)	9	-1.7	46.9	2.5	424.1	325.8	83.9	15	1.8	5.76
	Aso-4 distal ash-flow deposit (Miyazaki Pref.)	(PM)	5	-0.5	44.7	5.0	236.3	316.0	84.4	9	1.6	4.28
	Aso-4 co-ignimbrite ash-fall deposit	(AS)	17	-2.4	52.3	2.5	206.4	341.2	84.5	12	0.69	3.10
	(Chubu)		6	1.2	49.8	3.5	378.0	306.6	85.0	10	0.86	3.05
	(Tohoku)		8	-5.6	51.9	3.7	224.9	0.9	82.9	12	0.75	4.20
	(Hokkaido)		3	-1.2	57.9	5.4	523.8	334.4	84.7	16	0.17	0.270

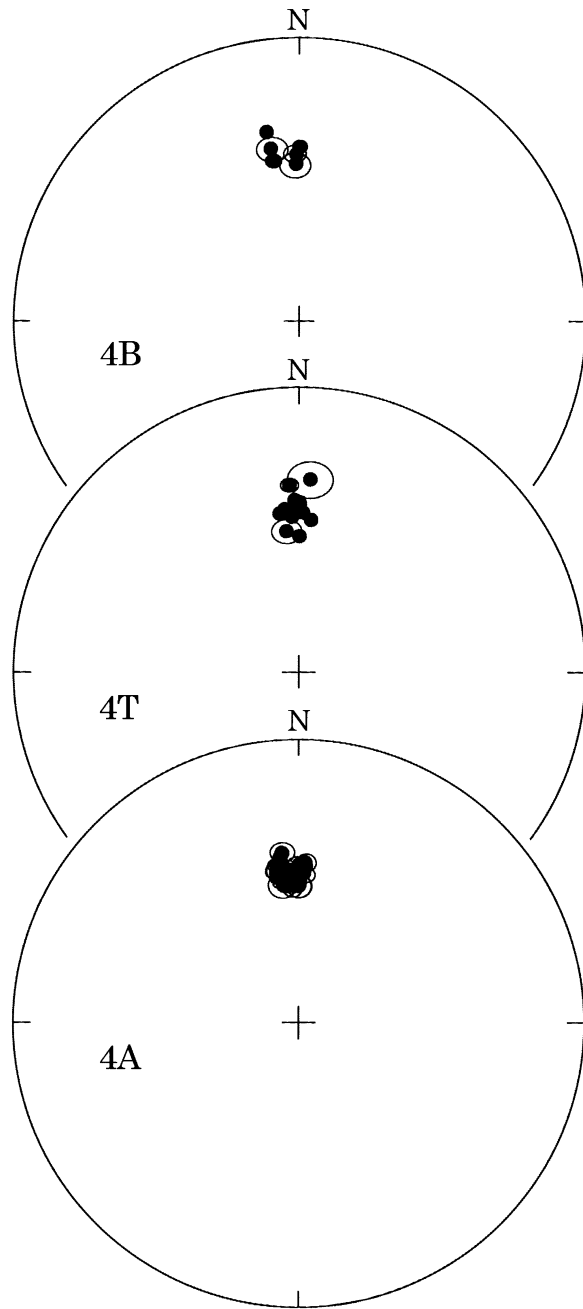*Aso-4A welded tuff, Aso-4A non-welded pyroclastic-flow deposit, and Yame clay.

FIGURE 18. Equal-area projection of 'geographically corrected site-mean directions'(corrected directions) and 95% confidence circles (lower hemisphere) for the Aso-4 pyroclastic-flow deposit. The corrected directions are calculated from their VGPs at a reference point in Aso caldera (131˚E, 33˚N). 4A: Aso-4A, Yame clay, and PYL, 4T: Aso-4T and PYU, 4B: Aso-4B.

dipole field was assumed to be located at the overall-mean VGP (104.6˚W , 81.1˚N, $A_{95} = 1.3˚$, N = 44). (2) The direction (declination, inclination) of the dipole field (DF) in each region was calculated using the overall-mean VGP, and the isogonic and isoclinic lines were drawn over the map of the Japanese Islands. The declinations and inclinations over the Japanese islands ranged between 8˚ and 10˚E, and between 45˚ and 55˚, respectively (Figs. 1 and 2). (3) The surveyed area was divided into 10 regions. A representative point in each region was supposed to locate the mean longitude and latitude of the sampling sites in each region. (4) The local geomagnetic field (LF) direction at the representative point was calculated using each regional-mean VGP. (5) The declination and inclination differences between LF and DF in each region were shown by numbers adjacent to the representative points in the isogonic and isoclinic charts. Almost all of the differences were less than 3˚ except in the Okayama-Hiroshima and Toyama regions. Judging from the α_{95}s for their paleomagnetic results, it could be recognized that the LF direction was anomalous when the difference between DF and LF was 3˚ or more. The declination difference between LF and DF in the Okayama-Hiroshima region was –5.4˚, and the inclination difference in the Toyama region was 6.7˚. These anomalous differences in the two regions, exceeding the α_{95}s of the LF directions, might be caused by the non-dipole field in the regions.

In this study, the DF pole is assumed to coincide with the overall-mean VGP (22.7˚W, 83.8˚N, $A_{95} = 1.3˚$, N = 42) for Aso-4A, PM, PYL, and AS. Declinations and inclinations over the Japanese Islands calculated from the DF pole range between –3.5˚ and –1.5˚, and between 44.0˚ and 59.0˚, respectively (Figs. 21 and 22). The surveyed area was divided into eight regions: central Kyushu, southern Kyushu, Chugoku, Chubu-1, Chubu-2, Tohoku-1, Tohoku-2, and Hokkaido, and the LF direction of each region was calculated from the regional-mean VGP (Table 5). The differences in declination between DF and LF for Chubu-1 and Tohoku-1 are 4.6˚ and –4.6˚, respectively (Fig. 21). Since these differences in declination are not too small compared with the directional differences by the local geomagnetic anomalies (LAs) at the time AT erupted, the differences might indicate LAs in the regions. Their α_{95}s, however, are too large to conclude that the differences are caused by LAs. Consequently, LAs exceeding the α_{95}s could not be detected by comparing DF and LF in all of the eight regions. Perhaps the reason why LAs were not found in this study is because the data are too few. The AS samples were not collected from the Okayama-Hiroshima and Toyama regions where LAs were recognized at the time of the AT eruption. Therefore, it cannot be confirmed whether LAs at the time of the AT eruption had existed in the same regions at the time of Aso-4A eruption.

Hyodo et al. (1993) carried out a paleomagnetic study of samples taken from drill cores in the Inland Sea, Lake Yogo, and Lake Kizaki, and presented similar GSV curves for each
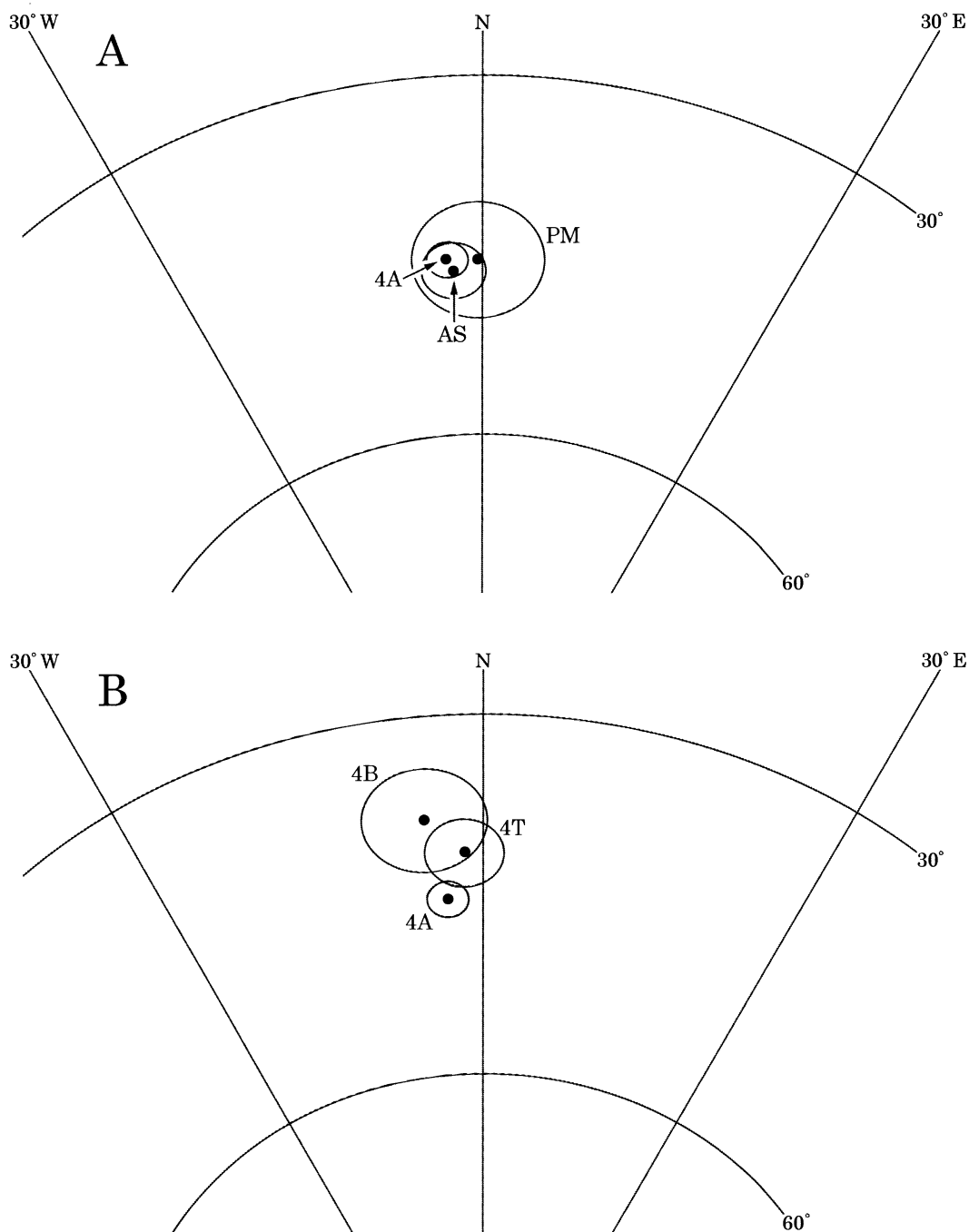
FIGURE 19. Equal-area projection of group-mean (or subunit-mean) corrected directions and 95% confidence circles (lower hemisphere) for the Aso-4 tephra (**A**: 4A, AS, and PM; **B**: 4A, 4T, and 4B). The corrected directions calculated from their VGPs at a reference point in Aso caldera (131°E, 33°N). 4A, 4T, and 4B are major stratigraphic groups in the area around Aso caldera. 4A: Aso-4A, Yame clay, and PYL, 4T: Aso-4T and PYU, 4B: Aso-4B, AS: the Aso-4 co-ignimbrite ash-fall deposit, PM: the Aso-4 distal ash-flow deposit in Miyazaki Prefecture.

A

B
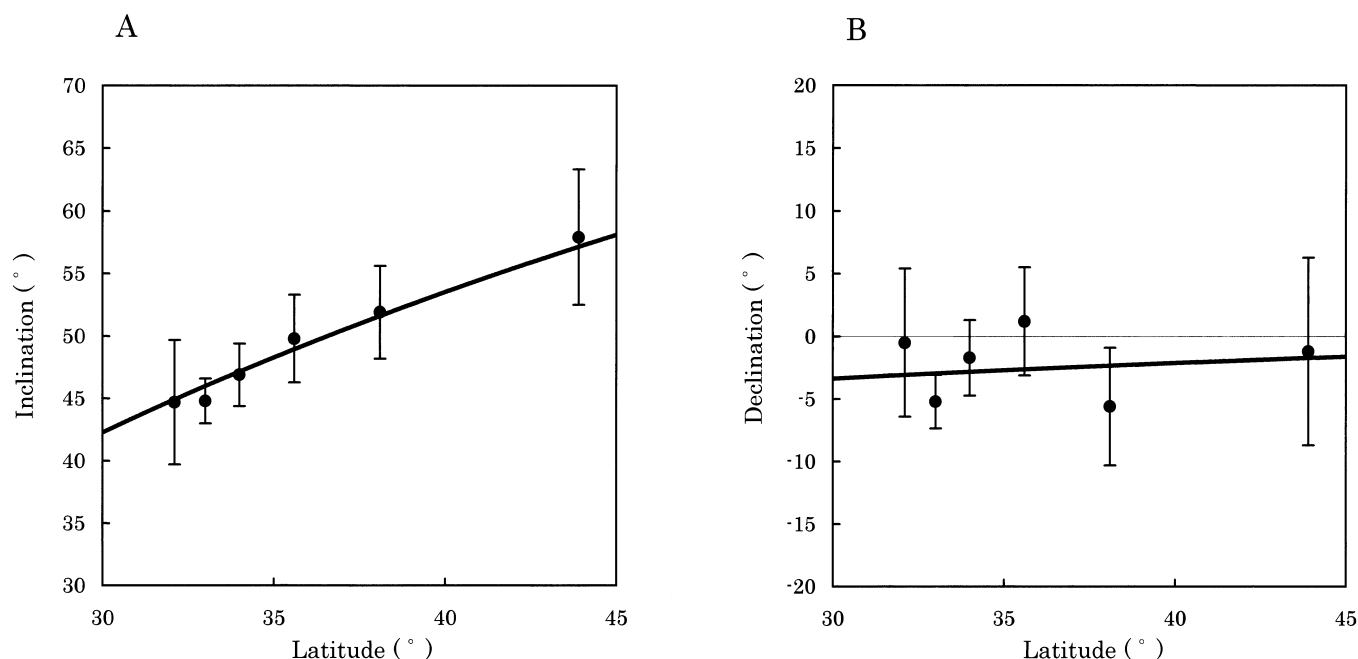
FIGURE 20. The relation between regional-mean directions (**A**: inclinations, **B**: declinations) and latitudes for paleomagnetic data correlated to the   Aso-4A eruption. Bold lines show the inclinations (**A**) and declinations (**B**) expected for the overall-mean VGP (22.7°W, 83.8°N). Error bars in inclinations and in declinations are α_{95} and α_{95}/cos (inclination), respectively.

region for the last 11,000 years. Moreover, Hayashida et al. (1996) showed that the paleomagnetic directions for two widespread tephras in three distant regions (central Kyushu, Kinki, and the Boso Peninsula) are identical within each correlative unit. These tephras occur at two different horizons dated at about 0.9 Ma and 1.0 Ma; they are the Imaich and the Yabakei pyroclastic-flow deposits in central Kyushu which produced widespread co-ignimbrite ashes that were emplaced in marine and non-marine sedimentary sequence over distances of up to 1,000 km. Judging from the present results and from the previous paleomagnetic reports, significant regional differences could not be observed in the configuration of the geomagnetic field throughout the Japanese Islands. Had LAs existed at the time of the Aso-4A eruption, they have been in the narrower zones than the eight regions of this study.

7. CONCLUSION

From the results of paleomagnetic measurements for the Aso pyroclastic-flow and the Aso-4 co-ignimbrite ash-fall deposits, following informations have been obtained.
1) The geomagnetic directions at the times of the Aso-1 and the Aso-4 eruptions were similar to that of the present geomagnetic field. On the other hand, the direction at the time of the Aso-2 eruption was characterized by a very steep inclination, and that of the Aso-3 eruption by an extremely

easterly by declination.
2) Magnetic minerals in the samples are chiefly magnetites or titanomagnetites, based on experimental results of stepwise ThD, IRM acquisition, and ThD of a three-component IRM.
3) The sampled subunits of the Aso-4 pyroclastic-flow deposit in the area around the source caldera are divided into three stratigraphic groups: 4A, 4T, and 4B in ascending order. The group-mean inclination of 4A is 6.7° steeper than that of 4B, and is 3.8° steeper than that of 4T. These inclination differences, in which the lower one is steeper than the upper, originated from the stratigraphic time gaps rather than from local geomagnetic anomalies. Assuming the directional differences were caused by GSV, the time interval between 4A and 4B can be estimated to be about 50 years or more based on the standard GSV curve for southwest Japan over the past 2,000 years.
4) The geomagnetic field at the time of the Aso-4A eruption is inferred to have been dominated by the same DF components in all regions of the Japanese Islands; the DF pole is assumed to coincide with the overall-mean VGP (22.7°W, 83.8°N). Had LAs existed at the time of the Aso-4A eruption, they have been in the narrower zones than the eight regions of this study.

Finally, the present and previous paleomagnetic studies regarding widespread tephras (Nakajima and Fujii, 1995a; Fujii and Nakajima, 1998) yielded the exact geomagnetic fields at the
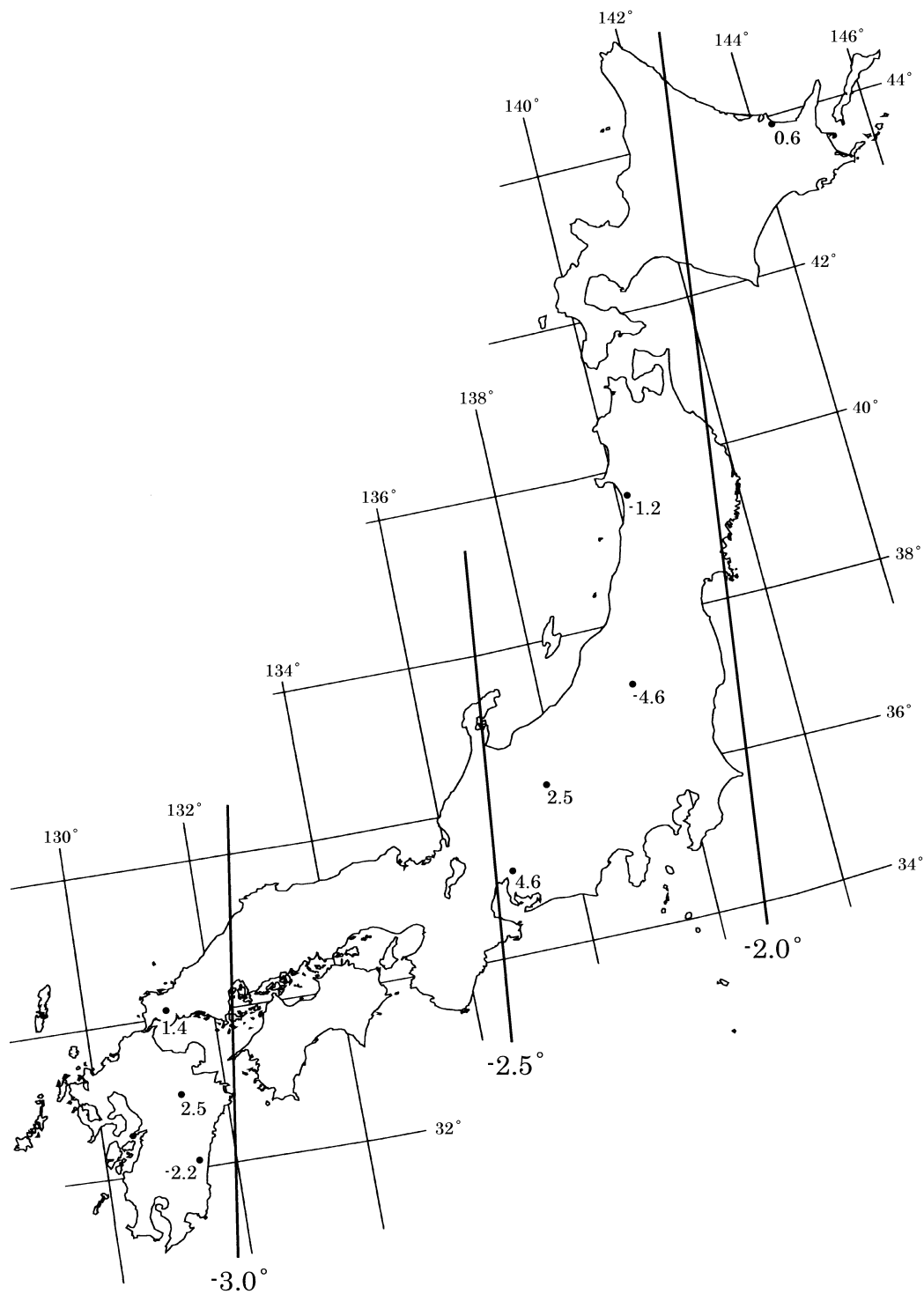
FIGURE 21. Isogonic chart at the time of the Aso-4A eruption. Isogonic lines are calculated from the overall-mean VGP. The surveyed area was divided into eight regions. Solid circles show representative points in the individual regions. Numbers adjacent to the solid circles show the values of D_1-D_2 in Table 5.
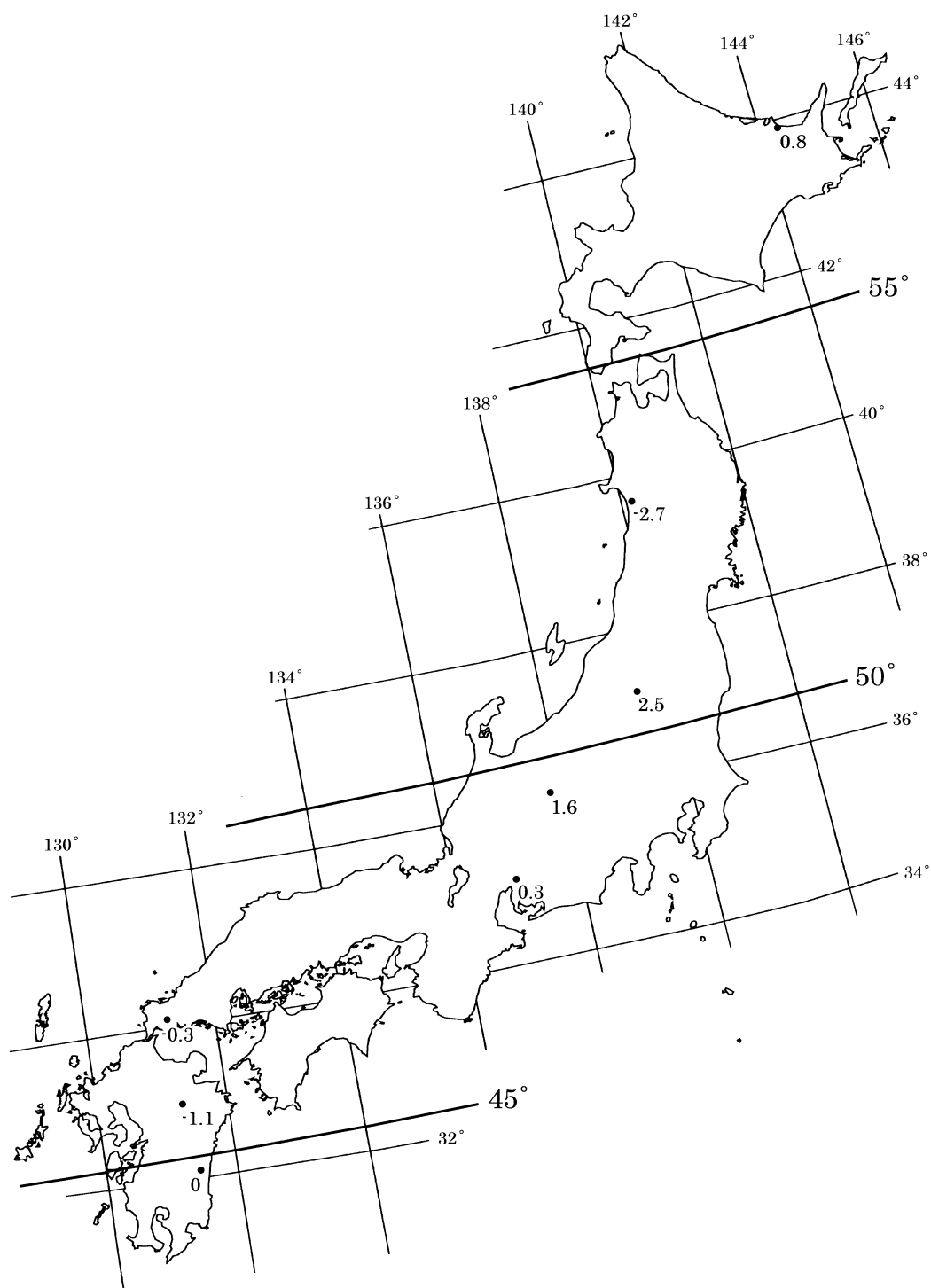
FIGURE 22. Isoclinic chart at the time of the Aso-4A eruption. Isoclinic lines are calculated from the overall-mean VGP. The surveyed area was divided into eight regions. Solid circles show representative points in the individual regions. Numbers adjacent to the solid circles show the values of I_1-I_2 in Table 5.

TABLE 5. Comparison of the local geomagnetic field (LF) with the inferred geomagnetic dipole field (DF). The DF pole is assumed to be located at the overall-mean VGP position (Lon. = 22.7°W, Lat. = 83.8°N, A_{95} = 1.3°, N = 42). The LF direction of individual regions was calculated from the regional-mean VGP (upper table). D_1 and I_1: declination and inclination of LF, D_2 and I_2: declination and inclination of DF.

Regional mean VGP

Region	Representative point		VGP			N	Site
	Lon. (° E)	Lat. (° N)	Lon. (° E)	Lat. (° N)	A_{95} (°)		
Central Kyushu	131.3	33.0	347.1	82.1	1.8	11	4A1-11
Southern Kyushu	131.4	32.1	316.0	84.4	4.3	5	PM1-5
Chugoku	131.3	34.1	325.8	83.9	2.7	9	PYL1-12
Chubu-1	137.0	35.1	298.9	84.2	7.2	3	AS4, 14, 15
Chubu-2	137.8	36.1	316.7	85.6	6.7	3	AS1-3
Tohoku-1	139.5	37.2	18.0	83.4	7.2	5	AS5-7, 16, 17
Tohoku-2	140.2	39.6	339.6	81.1	7.0	3	AS8, 12, 13
Hokkaido	144.3	43.9	334.4	84.7	6.2	3	AS9-11

Directions of the local and dipole field at the representative point

Region	LF		DF		D_1-D_2 (°)	I_1-I_2 (°)
	D_1 (° E)	I_1 (°)	D_2 (° E)	I_2 (°)		
Central Kyushu	-5.2	44.9	-3.0	46.0	-2.2	-1.1
Southern Kyushu	-0.5	44.9	-3.0	44.9	2.5	0
Chugoku	-1.7	47.0	-3.1	47.3	1.4	-0.3
Chubu-1	2.1	48.6	-2.5	48.3	4.6	0.3
Chubu-2	0.1	51.0	-2.4	49.4	2.5	1.6
Tohoku-1	-6.8	53.0	-2.2	50.5	-4.6	2.5
Tohoku-2	-3.4	50.4	-2.2	53.1	-1.2	-2.7
Hokkaido	-1.2	58.0	-1.8	57.2	0.6	0.8

times the tephras were deposited, based on the paleomagnetic results from multiple sites for individual tephras. It can be expected that GSV in the Quaternary would be completely elucidated by accumulating those data with high accuracy.

REFERENCES

Endo, H., and Y. Suzuki. 1986. Geology of the Tsuma and Takanabe district, with geological sheet map at 1:50,000 Geological Survey of Japan, 105 pp.*

Fisher, R. A. 1953. Dispersion on a sphere. Proc. Roy. Soc. A217: 295-305.

Fujii, J., and T. Nakajima. 1998. Paleomagnetic directions of Quaternary widespread tephras. Memoirs of the Faculty of Education, Fukui University, Series II 51: 47-60.*

Fujii, J., T. Nakajima and H. Kamata. 2001. Paleomagnetic directions of the Aso pyroclastic-flow and the Aso-4 co-ignimbrite ash-fall deposits in Japan. Earth, Planets and Space 53: 1137-1150.

Fujii, J., T. Nakajima, S. Ishida and S. Matsuo. 2000. Paleomagnetic directions of the Aso-4 tephra in Yamaguchi Prefecture, southwest Japan. The Quaternary Research (Japan) 39: 227-232.*

Gohara, Y., T. Shinbori, K. Suzuki, S. Nomura and C. Komori. 1964. Some problems on the Pleistocene formations of north Kyushu, Japan. Bull. Resource Res. Inst. 62: 83-108.*

Hayashida, A., H. Kamata and T. Danhara. 1996. Correlation of widespread tephra deposits based on paleomagnetic directions: link between a volcanic field and sedimentary sequences in Japan. Quaternary International 34-36: 89-98.

Hirooka, K. 1977. Recent trend in archaeomagnetic and palaeomagnetic studies in Quaternary research. The Quaternary Research (Japan) 15: 200-203.**

Hirooka, K. 1988. Paleomagnetic and archeomagnetic age dating. The Memoirs of the Geological Society of Japan 29: 305-318.*

Hoshizumi, H., K. Ono, K. Mimura and T. Noda. 1988. Geology of the Beppu district, with geological sheet map at 1:50,000. Geological Survey of Japan, 131 pp.*

Hyodo, M. 1999. Recent progress in paleomagnetic and rock-magnetic studies of the Quaternary in Japan. The Quaternary Research (Japan) 38: 202-208.

Hyodo, M., and S. Minemoto. 1996. Paleomagnetic dating using geomagnetic secular variations and excursions from lake sediments in Japan. The Quaternary Research (Japan) 35: 125-133.*

Hyodo, M., C. Itota and K. Yaskawa. 1993. Geomagnetic secular variation reconstructed from magnetizations of wide-diameter cores of Holocene sediments in Japan. Journal of Geomagnetism and Geoelectricity 45: 669-696.

Japan Association for Quaternary Research 1996. Inventory of Quaternary outcrops - Tephras in Japan -. Japan Association for Quaternary Research, 352 pp.**

Kamata, H. 1997. Geology of the Miyanoharu district, with geological sheet map at 1:50,000. Geological Survey of Japan, 127 pp.*

Kamata, H., A. Hayashida and T. Danhara. 1997. Identification of a pair of co-ignimbrite ash and underlying distal plinian ash in the Early Pleistocene widespread tephra in Japan. Journal of Volcanology and Geothermal Research 78: 51-64.

Kameyama, T. 1968. The Pleistocene formations of the Kammon district. The Journal of the Geological Society of Japan 74: 415-426.*

Kawai, N., K. Yaskawa, T. Nakajima, M. Torii and S. Horie. 1971. Oscillating geomagnetic field with a recurring reversal discovered from Lake Biwa. Proc. Japan Acad. 48: 186-190.

Kimura, J. 1996. Lacustrine Takano Formation at Takano, Shinko-cho, Nagano City; pp. 34-35 in Japan Association for Quaternary Research (ed.), Inventory of Quaternary outcrops - Tephras in Japan -. Japan Association for Quaternary Research.**

Kimura, K., T. Yoshioka, N. Imoto, S. Tanaka, M. Musashino and Y. Takahashi. 1998. Geology of the Kyoto-Tohokubu district, with geological sheet map at 1:50,000. Geological Survey of Japan, 89 pp.*

Kirschvink, J. L. 1980. The least-squares line and plane and the analysis of paleomagnetic data. Geophys. J. Roy. Astron. Soc. 62: 699-718.

Lowrie, W. 1990. Identification of ferromagnetic minerals in a rock by coercivity and unblocking temperature properties. Geophysical Research Letters 17: 159-162.

Machida, H. 1996. Widespread tephras including Aso-4 in lower part of the Fuji tephras at the eastern foot of Mt. Fuji; p. 36 in Japan Association for Quaternary Research (ed.), Inventory of Quaternary outcrops - Tephras in Japan -. Japan Association for Quaternary Research.**

Machida, H., and F. Arai. 1992. Atlas of tephra in and around Japan. University of Tokyo Press, 276 pp.**

Machida, H., F. Arai and M. Momose. 1985. Aso-4 ash: a widespread tephra and its implications to the events of late Pleistocene in and around Japan. Bulletin of the Volcanological Society of Japan, Second Series 30: 49-70.*

Matsumoto, A., K. Uto, K. Ono and K. Watanabe. 1991. K-Ar age determinations for Aso volcanic rocks - concordance with volcanostratigraphy and application to pyroclastic flows -. Abstracts of Fall Meeting in 1991, The Volcanological Society of Japan : 73.**

Nakajima, T., and J. Fujii. 1995a. Paleomagnetic direction of the Aira Tn tephra deposit. The Quaternary Research (Japan) 34: 297-307.*

Nakajima, T., and J. Fujii. 1995b. Magnetic susceptibilities of Quaternary tephras. Memoirs of Faculty of Education, Fukui University, Series II 47: 31-46.*

Nakajima, T., and J. Fujii. 1998. Paleomagnetic directions of the Aso-4 ash and the Aso pyroclastic flows. The Quaternary Research (Japan) 37: 371-383.*

National Astronomical Observatory. 1999. Rika Nenpyo (Chronological Scientific Tables 2000). Maruzen, 1064 pp.**

Okumura, K. 1991. Quaternary tephra studies in the Hokkaido district, northern Japan. The Quaternary Research (Japan) 30: 379-390.*

Okumura, K. 1996. Kutcharo pyroclastic-flow deposit IV in the southern region of Abashiri; p. 62 *in* Japan Association for Quaternary Research (ed.), Inventory of Quaternary outcrops - Tephras in Japan -. Japan Association for Quaternary Research.**

Ono, K. 1965. Geology of the eastern part of Aso caldera, central Kyushu, southwest Japan. The Journal of the Geological Society of Japan 71: 541-553.*

Ono, K. 1996a. Aso-3 pyroclastic-flow deposit along the Inaba river, Taketa City, Oita Prefecture; pp. 58-59 *in* Japan Association for Quaternary Research (ed.), Inventory of Quaternary outcrops - Tephras in Japan -. Japan Association for Quaternary Research.**

Ono, K. 1996b. Aso-1 pyroclastic-flow deposit in Taketa City, Oita Prefecture; pp. 68-69 *in* Japan Association for Quaternary Research (ed.), Inventory of Quaternary outcrops - Tephras in Japan -. Japan Association for Quaternary Research.**

Ono, K. 1996c. Aso-4 pyroclastic-flow deposit in the region southeast of Kujyu Volcano, Oita Prefecture; p. 33 *in* Japan Association for Quaternary Research (ed.), Inventory of Quaternary outcrops - Tephras in Japan -. Japan Association for Quaternary Research.**

Ono, K., and K. Watanabe. 1985. Geological map of Aso Volcano at 1:50,000. Geological Survey of Japan, 8 pp.*

Ono, K., Y. Matsumoto, M. Miyahisa, Y. Teraoka and N. Kambe. 1977. Geology of the Taketa district, with geological sheet map at 1:50,000. Geological Survey of Japan, 145 pp.*

Reynolds, R. L. 1979. Comparison of the TRM of the Yellowstone Group and the DRM of some Pearlette ash beds. Journal of Geophysical Research 84: 4525-4532.

Sakai, A., Y. Teraoka, K. Miyazaki, H. Hoshizumi and Y. Sakamaki. 1993. Geology of the Miemachi district, with geological sheet map at 1:50,000. Geological Survey of Japan, 115 pp.*

Shibuya, H., K. Hirata and S. Honjo. 1999. Paleomagnetic direction and intensity of the Aso-2 pyroclastic flow. Abstracts of Japan Earth and Planetary Science Joint Meeting: Ec-P017.**

Shiraishi, T., F. Arai and Y. Fujimoto. 1992. Discovery of Aso-4 ash and drift pumice of Aso-4 pyroclastic flow and Sambe-Kisuki pumice fall deposits in the upper Quaternary of the Oga Peninsula, Akita Prefecture, northeast Honshu, Japan. The Quaternary Research (Japan) 31: 21-27.*

Suzuki, T. 1993. Stratigraphy of middle Pleistocene tephra layers around Nasuno Plain, in north Kanto, central Japan. Journal of Geography 102: 73-90.*

Suzuki, T., J. Kimura, T. Soda, S. Chiba, M. Koarai, F. Arai, S. Yoshinaga and M. Takada. 1995. Identification of widespread tephras in and around Bandai Volcano, northeast Japan. Journal of Geography 104: 551-560.**

Teraoka, Y., K. Okumura, A. Murata and H. Hoshizumi. 1990. Geology of the Saiki district, with geological sheet map at 1:50,000. Geological Survey of Japan, 78 pp.*

Teraoka, Y., K. Miyazaki, H. Hoshizumi, T. Yoshioka, A. Sakai and K. Ono. 1992. Geology of the Inukai district, with geological sheet map at 1:50,000. Geological Survey of Japan, 129 pp.*

Toyokura, I., K. Ohmura, F. Arai, H. Machida, N. Takase, K. Nakadaira and T. Ito. 1991. Identification of the Sambe Kisuki tephra found in marine terrace deposits along costal areas of Hokuriku district, and its implications. The Quaternary Research (Japan) 30: 79-90.*

Watanabe, H., and Niigata Volcanic Ash Research Group. 1999. Tephrostratigraphy of loam formations in Niigata Prefecture. Daishiki 31: 19-29.**

Watanabe, K. 1978. Studies on the Aso pyroclastic flow deposits in the region to the west of Aso caldera, southwest Japan, I: Geology. The Memoirs of the Faculty of Education, Kumamoto University, Natural Science 27: 97-120.

Watson, G. S. 1956. Analysis of dispersion on a sphere. Mon. Not. Roy. Astron. Soc. Geophys. Supp. 7: 153-159.

Yagi, H., and T. Soda. 1989. A stratigraphical study on the late Pleistocene widespread tephras occurring in central and northern part of Miyagi Prefecture. Journal of Geography 98: 871-885.*

Yonezawa, H., Y. Uesugi and Kanto Quaternary Research Group. 1996. K-Tz and Aso-4 tephras in Tozurahara, Fujino-cho, Kanagawa Prefecture; p. 42 *in* Japan Association for Quaternary Research (ed.), Inventory of Quaternary outcrops - Tephras in Japan -. Japan Association for Quaternary Research.**

* : in Japanese with English abstract

**: in Japanese

1

1